

Appendices

Habitat heterogeneity and phenotypic variation: Site temperature largely predicts diverse spawning portfolios of an interior Chinook Salmon stock

20 October, 2025

Contents

A1 Datasets	2
A1.1 Spawn timing data	2
A1.2 Covariate Derivation and Screening	7
A2 Exploratory Data Analysis	10
A2.1 Bivariate relationships	10
A2.2 Stream temperature (temp_90)	12
A2.3 <code>mean_elevation</code>	14
A2.4 <code>slope</code>	15
A2.5 <code>flow_90</code>	17
A3 Data Anlaysis	20
A3.1 Initial Model Selection	20
A3.2 Targeted model comparison	23
A3.3 Interactions	25
A4 Model interpretation	26
A4.1 Model parameters and performance	26
A4.2 Residual diagnostics	27
A4.3 Predictions against original data	28
A4.4 Population-level effects	29
A4.5 Group-level effects (deviations from fixed effects)	34

A1 Datasets

A1.1 Spawn timing data

Spawn timing data for Chinook salmon were collected from 2001 to 2005 in the MFSR. Because redds were not observed daily, we inferred spawn dates as the initial date (day of year) a completed redd was observed. We removed data from 2001, and data from Knapp Creek and Cape Horn Creek, as these sites were not consistently sampled. The final dataset contained 3016 georeferenced redds (i.e., inferred spawn date) across 104 stream reaches (i.e., COMIDs), nested within six major spawning tributaries that also included Beaver Creek (tributary to Marsh Creek) and Elk Creek (tributary to Bear Valley Creek) to total eight different spawning streams, and spanning four years.

We spatially joined each redd GPS location to the NHDPlus Version 2 (Horizon Systems, 2018) to assign stream reaches based on a common identifier (COMID). The COMID is used to link redd data with covariate data associated with the stream reach on which it is located.

Grouping Structure

The structure of the data is repeated measures on COMIDs, and multiple years, shared across COMIDs within streams. Many COMIDs only have 1-2 observation (Figure A1.1). There are 23 COMIDs with <5 redds (26%), 13 with ≤ 2 . (12.5%).

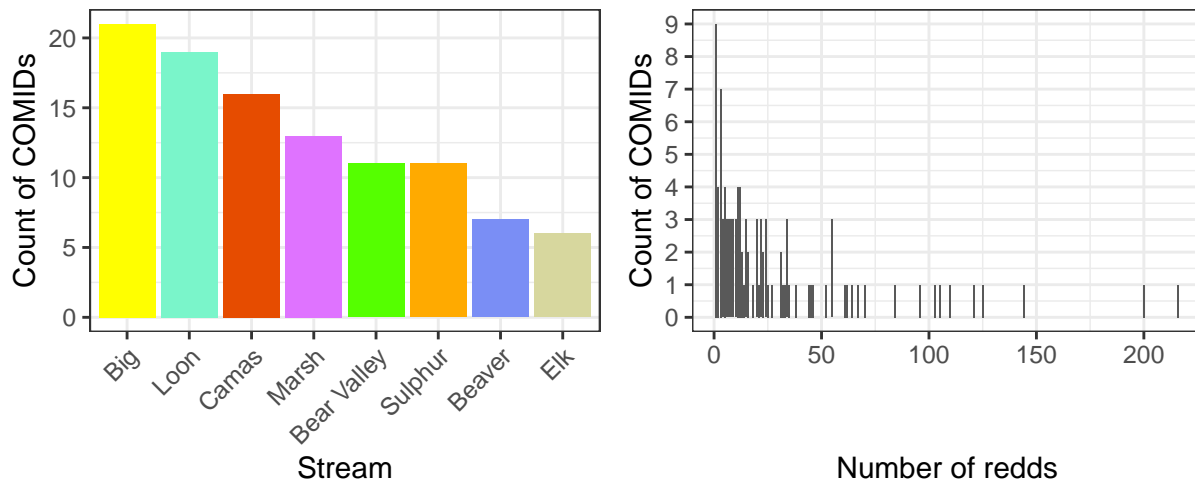


Figure A1.1: Number of observations (redds) per COMID.

Distribution of spawn timing

Spawn timing is generally unimodal, with a peak in late August to early September (Figure A1.2A). The distribution is slightly left skewed, but the mean and median are similar, indicating low skewness. The variance is low, suggesting no overdispersion. Suggests Poisson family for response if count of spawning events per day, or Gaussian if modeling day of year as continuous. There is also substantial variation in spawn date by stream and year (Fig. A1.2B-C; Fig. A1.3) and within COMIDs within streams (Fig. A1.4).

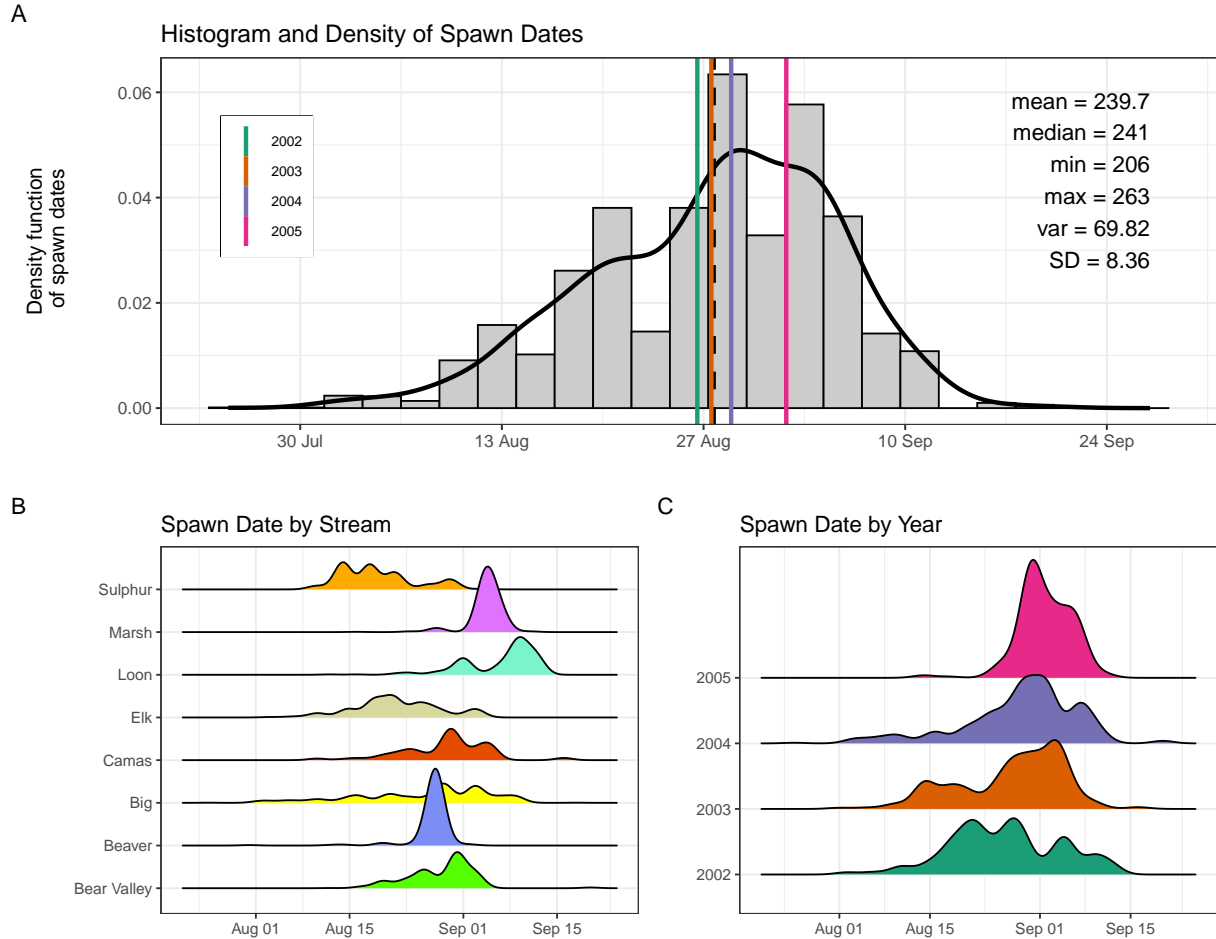


Figure A1.2: Histogram and density of spawn timing for all streams and years (A), and by stream (B) and year (C). In panel (A), colored, vertical lines indicate the mean spawn date for each year., and the black vertical line indicated the global mean.

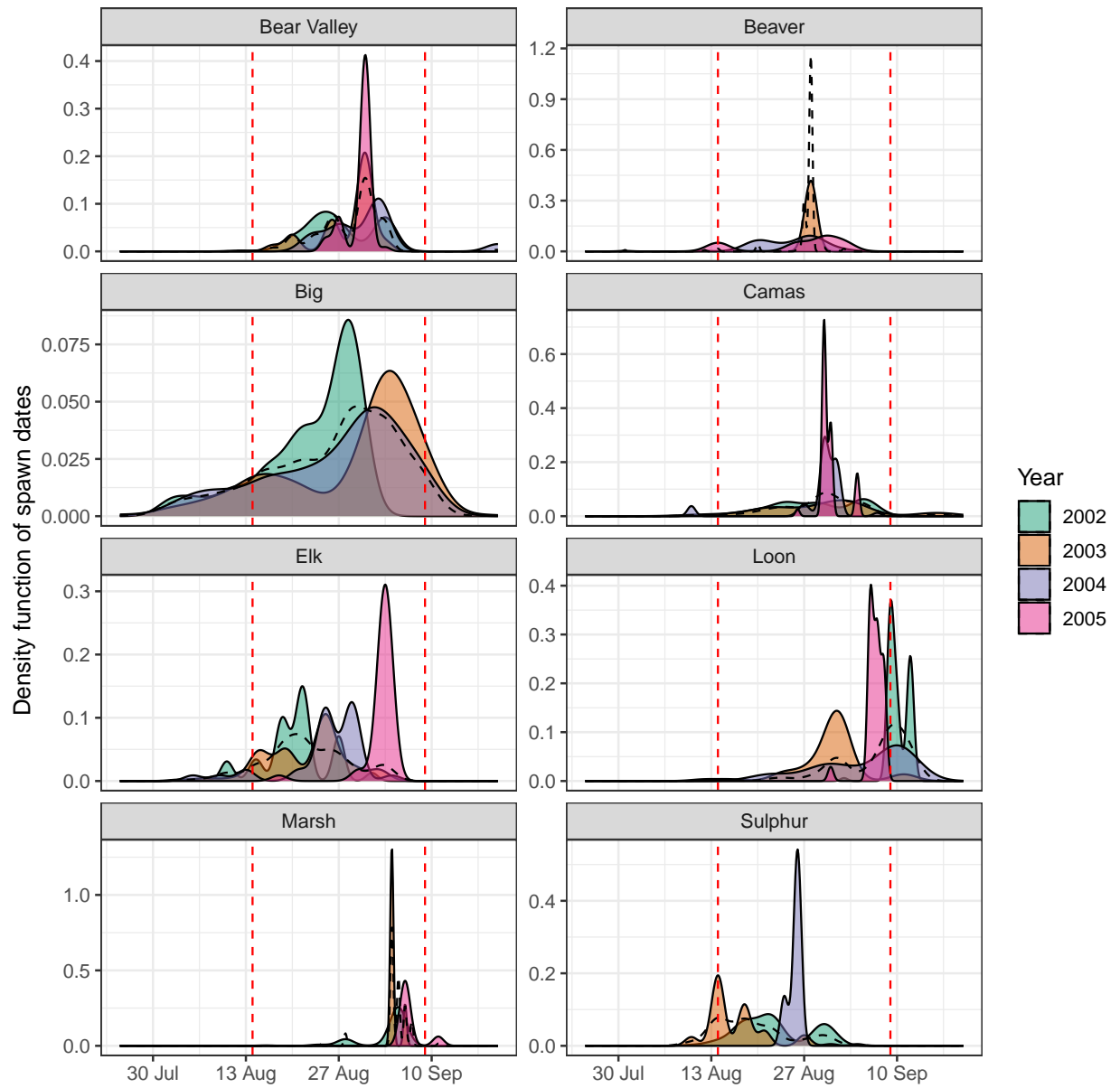


Figure A1.3: Histogram and density of Chinook salmon spawn timing across all streams and years (A), by stream (B), and by year (C). In panel (A), the histogram and kernel density illustrate the overall distribution of spawn dates; vertical-colored lines illustrate year-specific means, and the black line depicts the global mean. Spawn timing was generally unimodal, peaking in late August to early September.

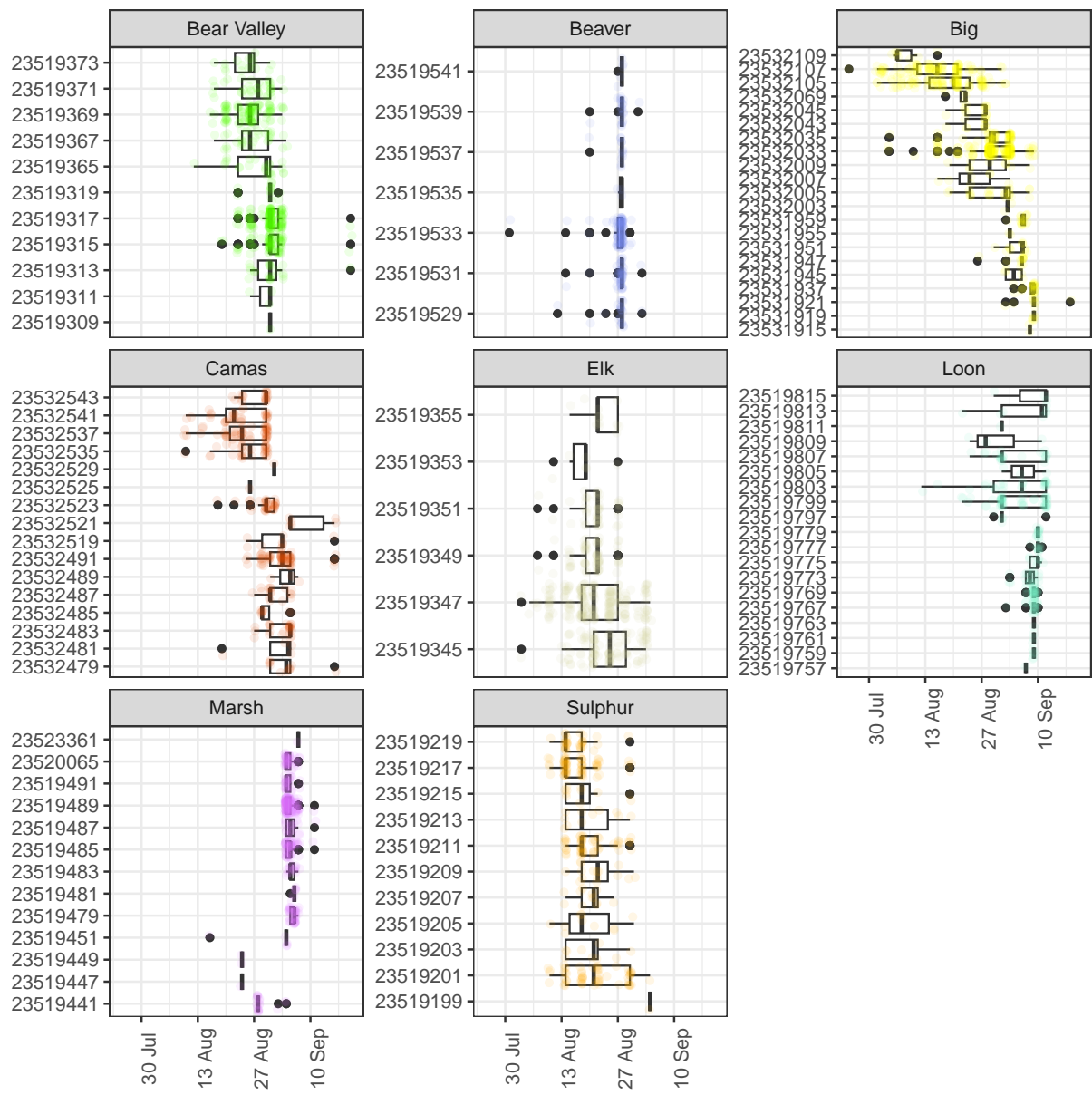


Figure A1.4: Variation in Chinooks salmon spawn timing by COMID within streams.

Cumulative proportion of redds over time

The temporal progression of Chinook salmon spawning activity varied within each stream across the four study years (Figure A1.5). The cumulative proportion of redds provides an intuitive measure of the spawning season's pace and timing. Streams like Marsh and Sulphur exhibit rapid increases, suggesting short, concentrated spawning windows. In contrast, streams like Big and Camas show more gradual increases, indicating a more protracted spawning season. Year-to-year variation is evident in several streams. Overall, this figure highlights both spatial and temporal heterogeneity in spawn timing that underpins the need for models incorporating stream- and year-specific effects.

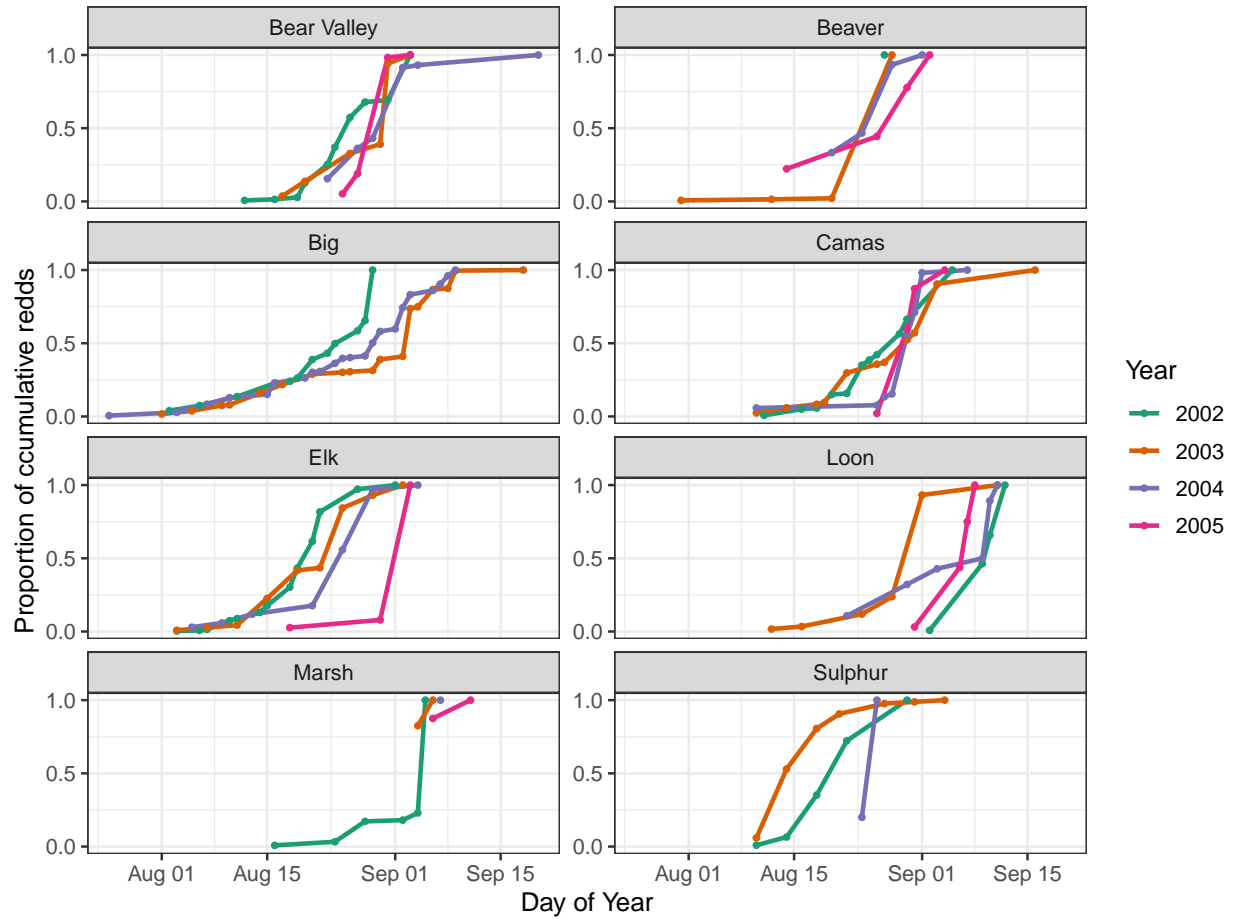


Figure A1.5: Proportion of cumulative Chinook salmon redds over time (day of year) across years (2002–2005) and streams. Each line represents a different year, with color denoting the year. Stream-specific panels illustrate temporal variation in the progression of spawning activity, as measured by cumulative redd counts normalized to the maximum value in each stream-year combination.

A1.2 Covariate Derivation and Screening

To identify environmental predictors of Chinook salmon spawn timing, we quantified covariates that describe thermal and physical stream conditions at redd locations. Covariates were selected based on three criteria: (1) demonstrated influence on salmon phenology in prior literature, (2) availability at all redd locations (i.e., COMIDs), and (3) low collinearity with other predictors.

The initial focal covariates included stream temperature ($^{\circ}\text{C}$), stream discharge (cms), elevation (m), and stream slope (unitless). Elevation and slope were extracted from NHDPlus (Moore et al. 2019).

Elevation and slope

Elevation and stream slope data were available at the COMID (stream reach) scale from the NHDPlus Version 2 (Horizon Systems, 2018).

Stream temperature

We used modeled daily average stream temperature values predicted at the stream segment (COMID) scale (Siegel et al. 2023). These data were downloaded and filtered to 2002-2005 and for the MFSR. Figure A1.6 shows the modeled thermal regimes for MFSR tributaries.

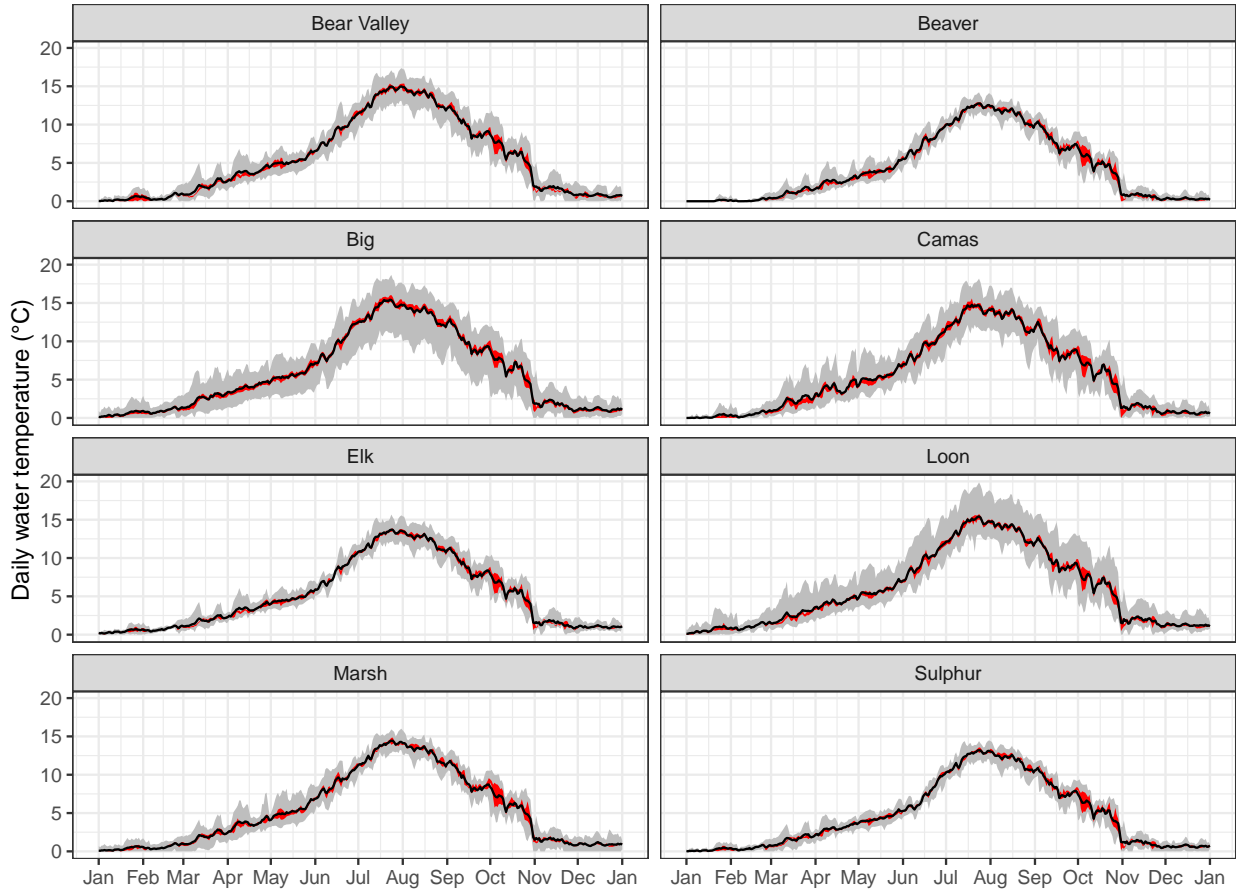


Figure A1.6: Modeled thermal regimes (2001-2005) for MFSR tributaries. Black line are means, Red ribbon are 40 to 60th percentiles, Grey ribbon are full range.

These modeled temperatures were validated against empirical logger data collected at a subset of sites in the Middle Fork basin, with strong agreement (Pearson correlation coefficient = 0.97; Figure A1.7).

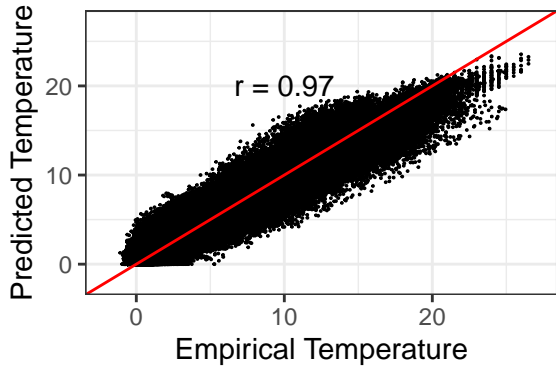


Figure A1.7: Comparison of modeled stream temperatures (Siegel et al. 2023) against empirical logger data for the Middle Fork Salmon River.

Discharge (streamflow)

Stream flow data were compiled from a single USGS Gage lower in the watershed (MF Salmon River at MF Lodge NR Yellow Pine ID - 13309220; Figure A1.8).

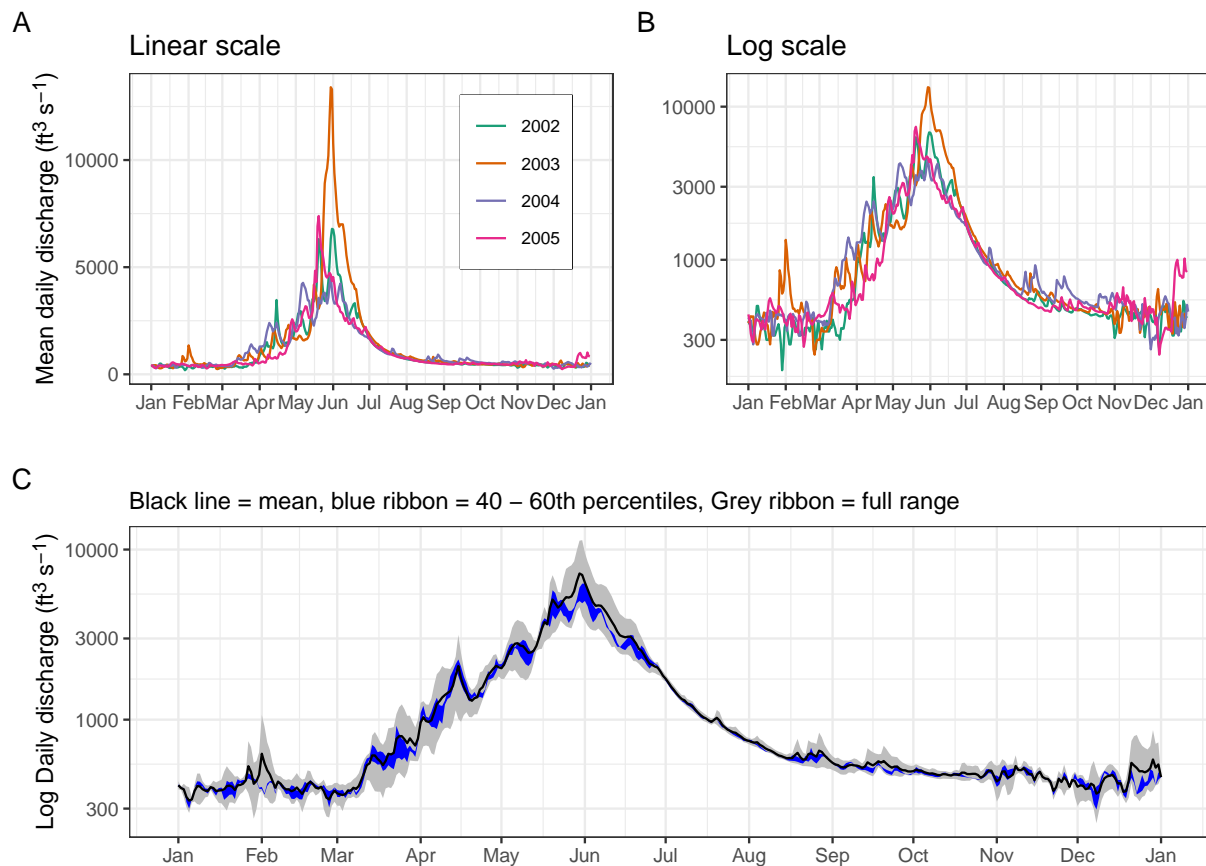


Figure A1.8: Inter-annual variability in daily discharge (cfs) at MF Lodge USGS Gage 13309220.

Time-windowed temp and flow metrics

For each redd, we computed several time-windowed summaries of temperature and flow relative to the inferred spawn date:

- *Antecedent metrics*: average conditions over 30, 60, and 90 days preceding the spawn date
- *Spanning metrics*: averages over time windows centered on the spawn date,
- *Post-spawn metrics*: 30-, 60-, and 90-day averages following the spawn date,
- *Time-invariant metrics*: summaries calculated relative to a fixed calendar date (e.g., August 1) representing an approximate onset of the spawning window.

The time invariant and after metrics were omitted from further consideration as preliminary data exploration showed weak if any relationship with spawn timing.

A2 Exploratory Data Analysis

A2.1 Bivariate relationships

We did exploratory data analysis on the compiled dataset to identify candidate covariates for inclusion in model selection. Bivariate relationships between spawn date (`yday`) and continuous predictors (Figure A2.1), and pairwise correlations between all continuous covariates (Figure A2.2), are shown below.

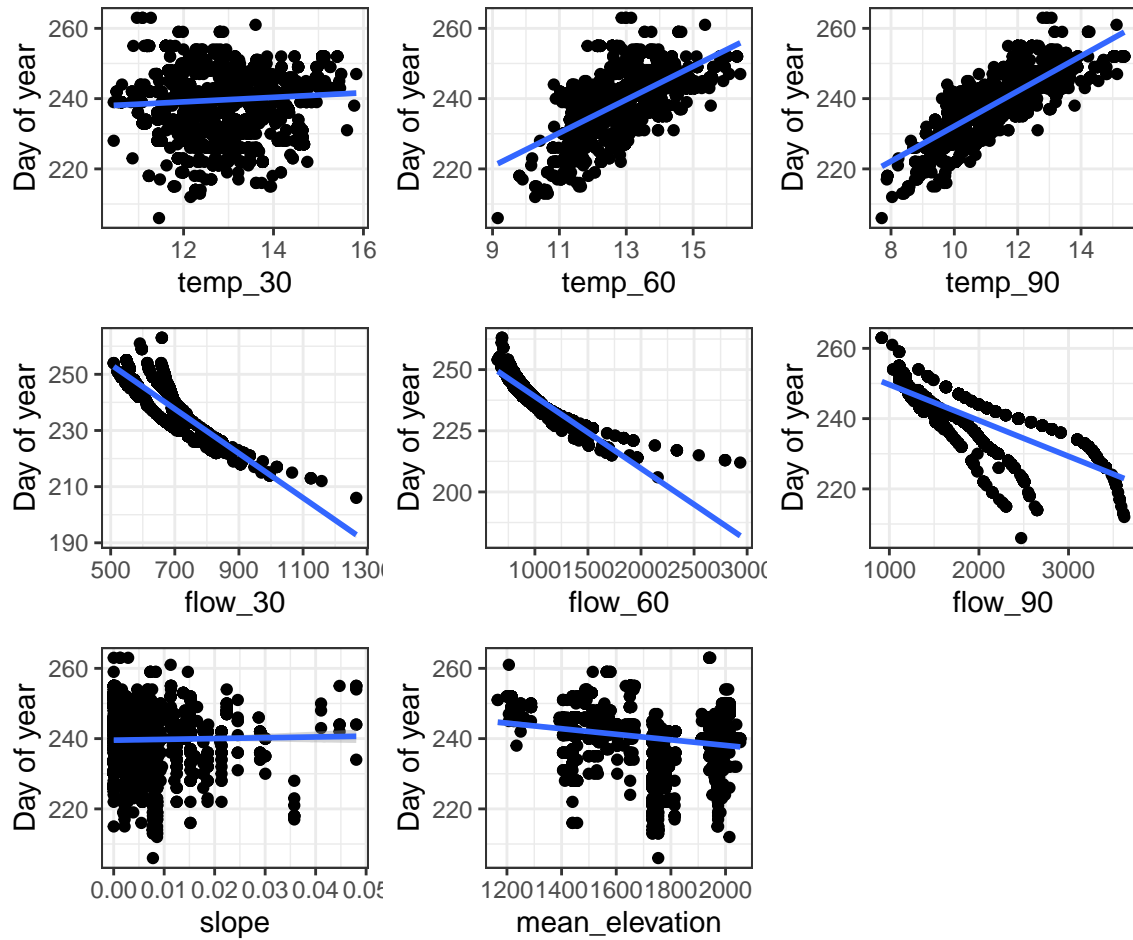


Figure A2.1: Bivariate relationships between spawn date ('yday') and continuous covariates. Solid lines are linear fits.

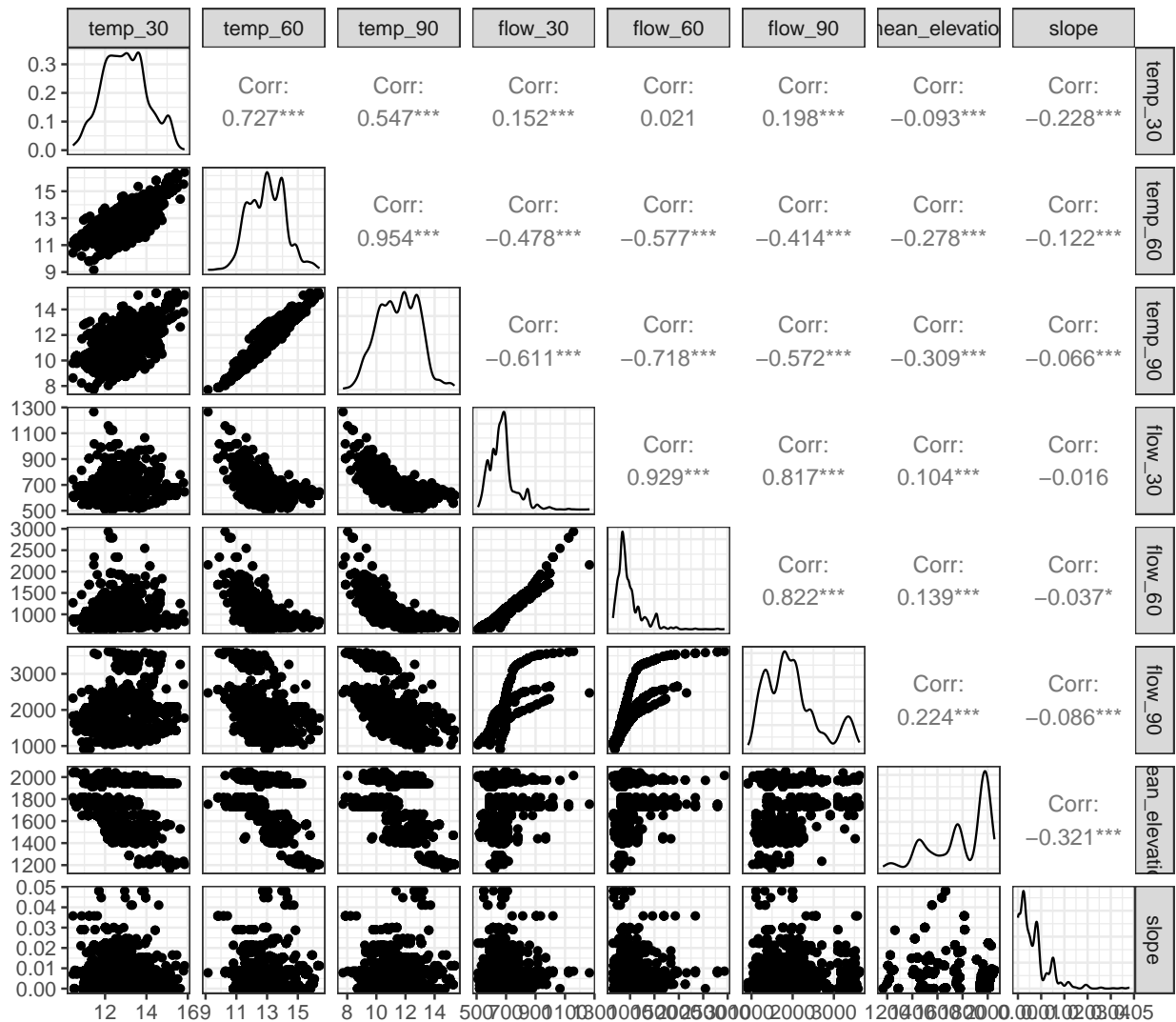


Figure A2.2: Pairwise correlations between continuous covariates.

Takeaways from Figures A2.1 and A2.2:

Among temperature variables, `temp_90` clearly shows the strongest relationship with spawn date (Figure A2.1), and is highly colinear with `temp_30` and `temp_60` (Figure A2.2).

The is a weak negative relationship between `mean_elevation` and `yday` (Figure A2.1), and it is weakly correlated with `temp_90` (0.31, Figure A2.2).

- `flow_30` = decaying exponential, obvious year effect
- `flow_60` = ditto
- `flow_90` = inflections, year effect clear
- `slope` = no relationship

A2.2 Stream temperature (temp_90)

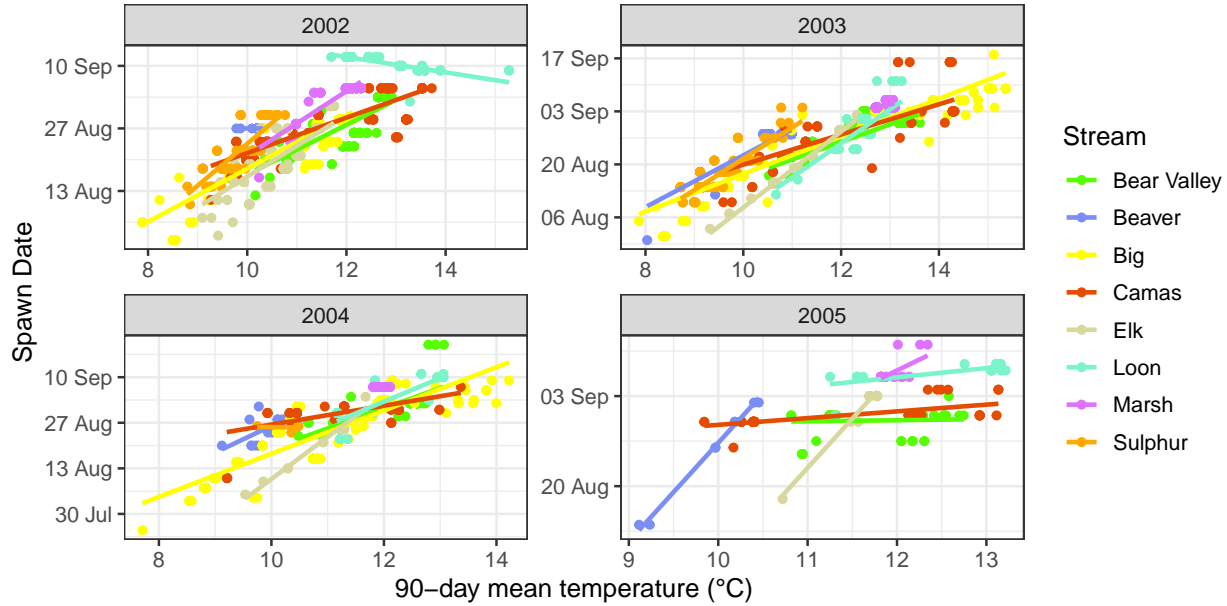


Figure A2.3: Relationship between 90 day antecedent stream temperature and spawn date by stream and year. Solid lines are linear fits.

Given observed positive relationships (Figure A2.3), we evaluated the role of `temp_90` in explaining variation in Chinook salmon spawn timing:

```
# temp_90 models
m.t90.1 <- lmer(yday ~ (1|COMID), data = df_mod, REML = FALSE)
m.t90.2 <- lmer(yday ~ temp_90 + (1|COMID), data = df_mod, REML = FALSE)
m.t90.3 <- lmer(yday ~ temp_90 + I(temp_90^2) + (1|COMID), data = df_mod, REML = FALSE)
```

The model with a quadratic effect of temperature (`m.t90.3`) improved dramatically over the null (intercept-only) model and linear effect (Table A2.1), and boosting both conditional and marginal R² (Table A2.2). This confirms a strong, nonlinear effect of pre-spawn temperature on spawn timing (Figure A2.4).

Table A2.1: AIC comparison of linear mixed models relating spawn date ('yday') to 'temp_90'.

Model	df	AIC	delta
m.t90.3	5	15848.81	0.0000
m.t90.2	4	16570.12	721.3107
m.t90.1	3	18629.30	2780.4987

Table A2.2: Model performance of linear mixed models relating spawn date ('yday') to 'temp_90'.

Name	R2_conditional	R2_marginal	ICC	RMSE	Performance_Score
m.t90.3	0.9177407	0.7643117	0.6509825	3.108315	0.8333333
m.t90.2	0.9086448	0.6915320	0.7038423	3.489863	0.6100606
m.t90.1	0.6571743	0.0000000	0.6571743	4.929494	0.0195227

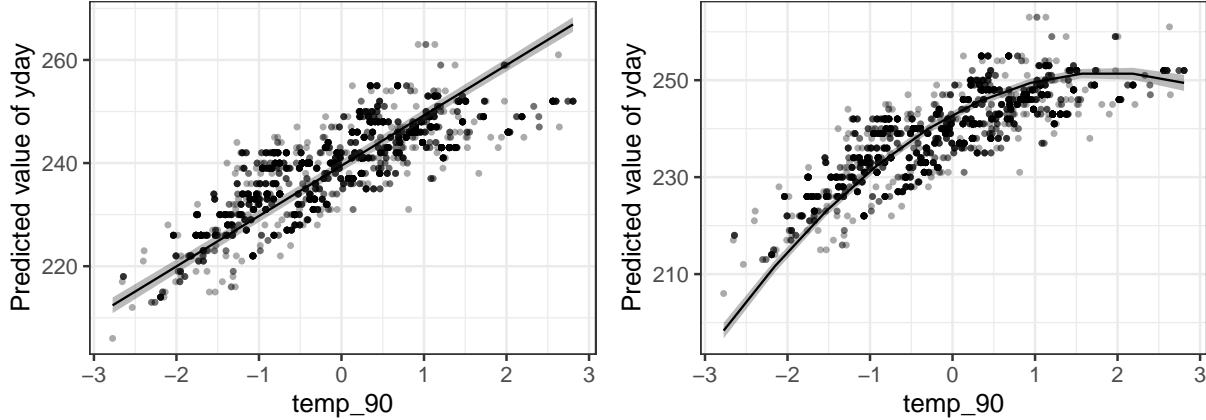


Figure A2.4: Marginal effect of 90 day antecedent stream temperature on spawn timing for (A) 'm.t90.2' and (B) 'm.t90.3'.

Next, we add in stream and year as main effects, and then interactions:

```
# temp + stream + year models
m.t90.4 <- lmer(yday ~ temp_90 + I(temp_90^2) + stream + (1|COMID), data = df_mod, REML = FALSE)
m.t90.5 <- lmer(yday ~ temp_90 + I(temp_90^2) + year + (1|COMID), data = df_mod, REML = FALSE)
m.t90.6 <- lmer(yday ~ temp_90 + I(temp_90^2) + stream + year + (1|COMID), data = df_mod, REML = FALSE)
m.t90.7 <- lmer(yday ~ temp_90 * stream + I(temp_90^2) + year + (1|COMID), data = df_mod, REML = FALSE)
m.t90.8 <- lmer(yday ~ temp_90 * year + I(temp_90^2) + stream + (1|COMID), data = df_mod, REML = FALSE)
```

Table A2.3: AIC comparison of linear mixed models relating spawn timing to temperature.

Model	df	AIC	delta
m.t90.8	18	12136.83	0.0000
m.t90.7	22	13038.01	901.1783
m.t90.6	15	13473.12	1336.2837
m.t90.5	8	13531.17	1394.3321
m.t90.4	12	15807.98	3671.1454
m.t90.3	5	15848.81	3711.9726

Adding stream (m.t90.4) or year (m.t90.5) individually improved model fit relative to m.t90.3, but year alone (m.t90.5) performed better than stream alone (m.t90.4) (Table A2.3).

Combining stream and year additively (m.t90.6) provided further improvement in AIC, along with the best marginal R2 and RMSE (Table A2.4). This suggests that both stream and year provide meaningful structure in explaining variation in spawn timing. Adding the interaction between temperature and stream (m.t90.7) increased complexity, slightly lowered the marginal R2, and has high multicollinearity (VIF ~ 15).

Table A2.4: Model performance of linear mixed models relating spawn timing to temperature.

Name	R2_conditional	R2_marginal	ICC	RMSE	Performance_Score
m.t90.8	0.9928189	0.6448836	0.9797782	1.581472	0.8333333
m.t90.7	0.9852284	0.7177821	0.9476590	1.865263	0.5267941
m.t90.6	0.9800601	0.7293886	0.9263154	2.022117	0.5061439
m.t90.5	0.9871140	0.6600787	0.9620912	2.021778	0.4528690
m.t90.3	0.9177407	0.7643117	0.6509825	3.108315	0.2196386
m.t90.4	0.8982595	0.7921275	0.5105629	3.110542	0.1666667

Adding the interaction between temperature and year (`m.t90.8`) gave the lowest AIC overall but had the lowest marginal R² of all models tested. This means that while the model “fit” the data better on paper (AIC), it did so by overfitting or by capturing year-to-year idiosyncrasies that may not generalize well to new data (suspicious marginal effect, Figure A2.5).

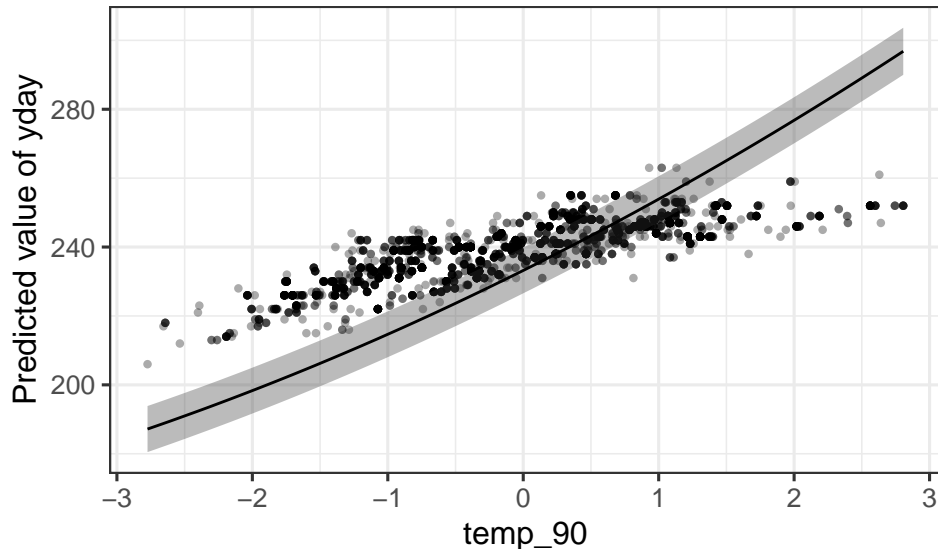


Figure A2.5: Marginal effect ('m.t90.8') of 90 day antecedent stream temperature on spawn timing.

The suspicious curvature in the marginal effect plot of `m.t90.8` (showing an unrealistic predicted relationship between `temp_90` and `yday`) confirms the risk of confounding or overfitting with interaction terms—particularly given that the random intercepts already capture substantial site-level variation.

Given the trade-offs, model `m.t90.6` emerged as the best compromise: it retained additive main effects of temperature, stream, and year, had high conditional and marginal R², moderate AIC, low RMSE, and avoided high multicollinearity.

A2.3 mean_elevation

Figure A2.6 shows the relationship between (A) `mean_elevation` and `temp_90` by stream and (B) `mean_elevation` and `yday` (spawn date) by stream and year.

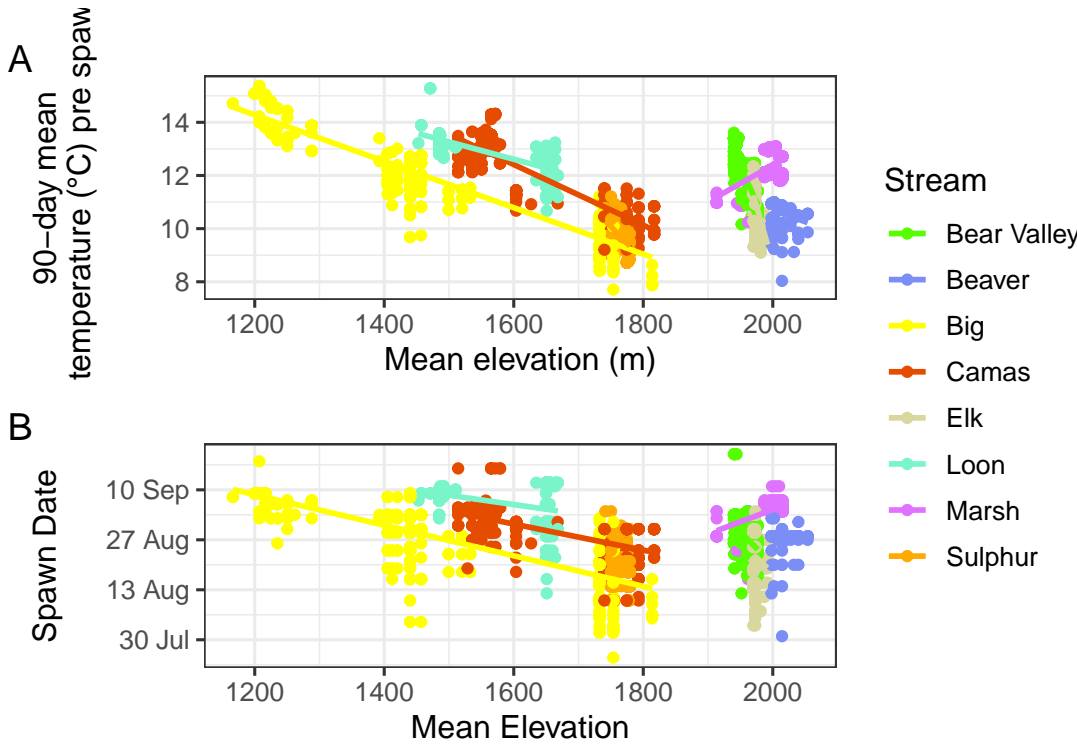


Figure A2.6: Relationship between (A) mean_elevation and temp_90 by stream and (B) mean_elevation and spawn timing by stream and year. Solid lines are linear fits.

We evaluated the role of mean elevation in explaining variation in Chinook salmon spawn timing:

```
# mean elevation models
m.ele.1 <- lmer(yday ~ (1|COMID), data = df_mod, REML = FALSE)
m.ele.2 <- lmer(yday ~ mean_elevation + (1|COMID), data = df_mod, REML = FALSE)
m.ele.3 <- lmer(yday ~ mean_elevation + stream + (1|COMID), data = df_mod, REML = FALSE)
m.ele.4 <- lmer(yday ~ mean_elevation + year + (1|COMID), data = df_mod, REML = FALSE)
m.ele.5 <- lmer(yday ~ mean_elevation + stream + year + (1|COMID), data = df_mod, REML = FALSE)
m.ele.6 <- lmer(yday ~ mean_elevation * stream + (1|COMID), data = df_mod, REML = FALSE)
m.ele.7 <- lmer(yday ~ mean_elevation * year + (1|COMID), data = df_mod, REML = FALSE)
```

Including mean elevation as a main effect improved model fit ($\Delta\text{AIC} = 19$ between `m.ele.1` and `m.ele.2`). The best-supported model (`m.ele.5`) included mean elevation alongside stream and year ($\Delta\text{AIC} = 281$ between `m.ele.2` and `m.ele.5`), with moderate collinearity (VIFs ~ 6), suggesting that mean elevation can contribute to explaining spawn timing when controlling for stream and year.

However, adding interactions with stream or year substantially increased model complexity and collinearity, as evidenced by extremely high VIFs (>45). Given the known inverse relationship between elevation and temperature across streams (Figure A2.6A), caution is warranted when later incorporating both elevation and temperature in the same model.

A2.4 slope

`slope` is not related to `yday` (Figure A2.7A), though there is some association between `slope` and `yday` when considering stream (Figure A2.7B). We will likely drop `slope`.

Table A2.5: AIC comparison of linear mixed models relating spawn timing to mean_elevation.

Model	df	AIC	delta
m.ele.5	14	18329.29	0.00000
m.ele.6	18	18371.62	42.33148
m.ele.3	11	18431.88	102.58771
m.ele.7	10	18435.12	105.82567
m.ele.4	7	18501.44	172.14764
m.ele.2	4	18611.27	281.97710
m.ele.1	3	18629.30	300.01337

Table A2.6: Model performance of linear mixed models relating spawn timing to mean_elevation.

Name	R2_conditional	R2_marginal	ICC	RMSE	Sigma	AICc_wt	Performance_Score
m.ele.5	0.6399737	0.5939968	0.1132428	4.876512	4.927506	1	0.6843974
m.ele.7	0.6684326	0.1243275	0.6213568	4.774852	4.851946	0	0.5175646
m.ele.4	0.6574860	0.1155940	0.6127186	4.835441	4.913296	0	0.4006749
m.ele.1	0.6571743	0.0000000	0.6571743	4.929494	5.009972	0	0.2596896
m.ele.2	0.6503692	0.1014398	0.6108988	4.929830	5.009158	0	0.2505245
m.ele.6	0.6398941	0.6301923	0.0262347	4.989054	5.016809	0	0.1678027
m.ele.3	0.6269782	0.5838335	0.1036716	4.971609	5.022058	0	0.1413263

Table A2.7: Variance inflation factors for model m.ele.5.

	GVIF	Df	$\text{GVIF}^{(1/(2*Df))}$
mean_elevation	5.739424	1	2.395709
stream	5.943076	7	1.135760
year	1.042077	3	1.006893

Table A2.8: Variance inflation factors for model m.ele.6.

	GVIF	Df	$\text{GVIF}^{(1/(2*Df))}$
mean_elevation	2.317261e+03	1	48.137937
stream	9.622172e+10	7	6.088629
mean_elevation:stream	5.226657e+11	7	6.870938

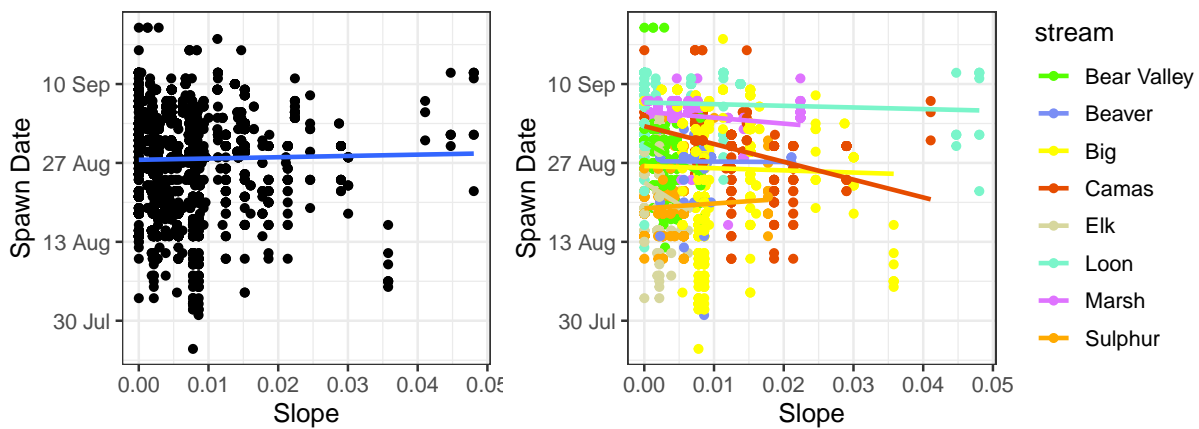


Figure A2.7: Bivariate relationship between ‘slope’ and spawn date (A) and by stream (B). Solid lines are linear fits.

A2.5 flow_90

Because flow data are not COMID- or stream-specific, it makes sense to think about and represent flow as an out-of-basin year effect that determines when adults make it back to the MFSR and initially onto the spawning grounds. The strong correlation between `flow_90` and `year` can be seen clearly in (Figure A2.8A).

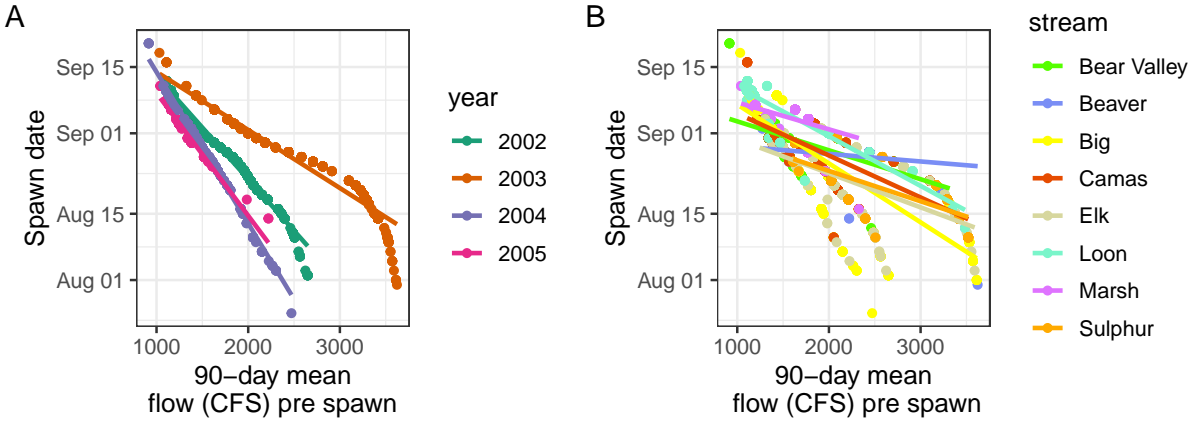


Figure A2.8: Spawn timing vs. 90-day mean discharge pre spawn at MF Lodge.

Next we compare the following simple linear models to examine functional structure:

```
# flow_90 models
m.flow.1 <- lm(yday ~ flow_90, data = model_data)
m.flow.2 <- lm(yday ~ I(flow_90^2), data = model_data)
m.flow.3 <- lm(yday ~ flow_90 + year, data = model_data)
m.flow.4 <- lm(yday ~ flow_90 + year + stream, data = model_data)
m.flow.5 <- lm(yday ~ flow_90 * stream, data = model_data)
m.flow.6 <- lm(yday ~ flow_90 * stream + year, data = model_data)
m.flow.7 <- lm(yday ~ flow_90 * year + stream, data = model_data)
m.flow.8 <- lm(yday ~ flow_90 * stream + I(flow_90^2), data = model_data)
m.flow.9 <- lm(yday ~ flow_90 * stream + year + I(flow_90^2), data = model_data)
```

Table A2.9: Model performance of linear models relating spawn date ('yday') to 'flow_90'.

Name	R2	R2_adjusted	RMSE	Sigma	AICc_wt	Performance_Score
m.flow.7	0.9780529	0.9779505	1.237710	1.240800	1	1.0000000
m.flow.9	0.9407030	0.9403269	2.034449	2.041229	0	0.4960534
m.flow.6	0.9108990	0.9103638	2.493858	2.501751	0	0.4472891
m.flow.4	0.8913935	0.8909958	2.753330	2.758824	0	0.4181935
m.flow.3	0.8745347	0.8743681	2.959322	2.961778	0	0.3942842
m.flow.8	0.7348812	0.7334668	4.301804	4.313980	0	0.2174139
m.flow.5	0.7130109	0.7115760	4.475722	4.487641	0	0.1921569
m.flow.1	0.5900974	0.5899614	5.348977	5.350752	0	0.0576227
m.flow.2	0.5352432	0.5350890	5.695650	5.697539	0	0.0000000

Table A2.10: Parameter estimates for m.flow.7

Parameter	Coefficient	SE	CI_low	CI_high	p
(Intercept)	278.2566486	0.2130585	277.8388932	278.6744041	0.0000000
flow_90	-0.0219390	0.0001136	-0.0221617	-0.0217163	0.0000000
year2003	-8.3607844	0.2371172	-8.8257131	-7.8958557	0.0000000
year2004	11.0240656	0.3856186	10.2679620	11.7801692	0.0000000
year2005	1.0123700	0.7619753	-0.4816766	2.5064167	0.1840768
streamBeaver	0.5591186	0.1048594	0.3535151	0.7647220	0.0000001
streamBig	-0.4395848	0.0772852	-0.5911220	-0.2880475	0.0000000
streamCamas	-0.0934454	0.0899470	-0.2698094	0.0829186	0.2989375
streamElk	0.2219142	0.0861007	0.0530918	0.3907365	0.0100026
streamLoon	0.0895360	0.1073905	-0.1210304	0.3001024	0.4044923
streamMarsh	-0.7143977	0.0913025	-0.8934196	-0.5353759	0.0000000
streamSulphur	-0.0665471	0.1017872	-0.2661269	0.1330327	0.5132997
flow_90:year2003	0.0094506	0.0001190	0.0092172	0.0096840	0.0000000
flow_90:year2004	-0.0101387	0.0002436	-0.0106163	-0.0096610	0.0000000
flow_90:year2005	-0.0046105	0.0005766	-0.0057411	-0.0034799	0.0000000

Collinearity

High collinearity (VIF) may inflate parameter uncertainty

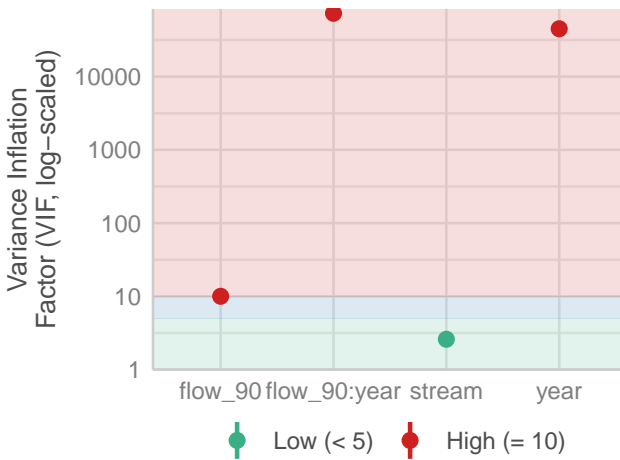


Figure A2.9: Variance inflation factors for model m.flow.7

AIC scores suggest `m.flow.7` is best model (Table A2.9). However, while the R^2 value is 0.98, the parameter estimate for `flow_90` has an incredibly small standard error and most variation is now attributed to the year contrasts (Table A2.10). Thus, `flow_90` is clearly confounded with `year`, and confirmed by high Variance Inflation Factor (VIF) scores (Figure A2.9).

A2.5.1 Why `flow_90` is problematic

Not spatially resolved

- We are modeling spawn timing at the redd level (COMID/stream)
- But `flow_90` is calculated from a single downstream gauge, and applied to all redds

- This assumes flow conditions are identical across all sites
- Including it gives the illusion of spatially resolved variation that isn't there

Correlated with year

- Since `flow_90` varies mostly across years, it is strongly confounded with year
- Any flow-related signal is probably already captured by your year fixed effect
- Including both `flow_90` and year risks collinearity, and may produce misleading inferences

Spawn-time aligned flow does not equal experienced flow

- While `flow_90` is aligned to each redd's spawn date, it still reflects a lower-basin gauge, not the actual hydrologic conditions experienced at the redd site
- So it might be precisely wrong — aligned in time but irrelevant in space

Recommendation: Drop `flow_90` from model.

Although we initially considered including 90-day mean streamflow (`flow_90`) as a predictor of spawn timing, this variable was ultimately excluded due to concerns about ecological validity and model overfitting. Stream flow data were derived from a single downstream USGS gauge and did not capture spatial variation across the study streams or reaches. Moreover, because `flow_90` was closely aligned with year, it introduced strong collinearity with the year effect and risked attributing site-level variation to flow patterns not actually experienced by individual redds. As such, we excluded `flow_90` to avoid misleading inference.

A3 Data Analysis

The final analysis dataset includes:

- `yday`: spawn date, continuous response variable
- `comid`, `stream`, `year`: grouping variables
- `temp_90`: 90-day mean temperature pre-spawn, continuous predictor variable
- `slope` and `mean_elevation`: provisionally retaining continuous predictor variable

We used linear mixed-effects models to evaluate environmental predictors of Chinook salmon spawn timing, with redd observation day-of-year (`yday`) as the response variable. We scaled the continuous covariates to have a mean of 0 and standard deviation of 1 to assist convergence and interpretation. COMID will be included in all models as a random (intercept) effect to account for repeated measures on COMIDs. Stream will be treated as a fixed effect to compare average effects across streams, and `year` as a fixed effect to compare average effects across years. Further, based on exploratory analysis and biological expectations of nonlinear thermal responses, temperature effects were modeled using both linear and quadratic terms for the 90-day average stream temperature prior to spawning (`temp_90` and `I(temp_90^2)`).

A3.1 Initial Model Selection

We fit 31 additive models representing all combinations of fixed effects: `temp_90`, `stream`, `year`, `slope`, and `mean_elevation`. Model selection was performed using AIC, and model fit was evaluated using marginal and conditional R², RMSE, and intraclass correlation coefficients (ICC).

```
# one covariate
m1 <- lmer(yday ~ temp_90 + I(temp_90^2) + (1 | COMID), data = df_mod,
            REML = FALSE)
m2 <- lmer(yday ~ stream + (1 | COMID), data = df_mod, REML = FALSE)
m3 <- lmer(yday ~ year + (1 | COMID), data = df_mod, REML = FALSE)
m4 <- lmer(yday ~ mean_elevation + (1 | COMID), data = df_mod, REML = FALSE)
m5 <- lmer(yday ~ slope + (1 | COMID), data = df_mod, REML = FALSE)

# two covariates
m6 <- lmer(yday ~ temp_90 + I(temp_90^2) + stream + (1 | COMID), data = df_mod,
            REML = FALSE)
m7 <- lmer(yday ~ temp_90 + I(temp_90^2) + year + (1 | COMID), data = df_mod,
            REML = FALSE)
m8 <- lmer(yday ~ temp_90 + I(temp_90^2) + mean_elevation + (1 | COMID),
            data = df_mod, REML = FALSE)
m9 <- lmer(yday ~ temp_90 + I(temp_90^2) + slope + (1 | COMID), data = df_mod,
            REML = FALSE)
m10 <- lmer(yday ~ stream + year + (1 | COMID), data = df_mod, REML = FALSE)
m11 <- lmer(yday ~ stream + mean_elevation + (1 | COMID), data = df_mod,
            REML = FALSE)
m12 <- lmer(yday ~ stream + slope + (1 | COMID), data = df_mod, REML = FALSE)
m13 <- lmer(yday ~ year + mean_elevation + (1 | COMID), data = df_mod,
            REML = FALSE)
m14 <- lmer(yday ~ year + slope + (1 | COMID), data = df_mod, REML = FALSE)
m15 <- lmer(yday ~ mean_elevation + slope + (1 | COMID), data = df_mod,
            REML = FALSE)

# three covariates
```

```

m16 <- lmer(yday ~ temp_90 + I(temp_90^2) + stream + year + (1 | COMID),
  data = df_mod, REML = FALSE)
m17 <- lmer(yday ~ temp_90 + I(temp_90^2) + stream + mean_elevation + (1 |
  COMID), data = df_mod, REML = FALSE)
m18 <- lmer(yday ~ temp_90 + I(temp_90^2) + stream + slope + (1 | COMID),
  data = df_mod, REML = FALSE)
m19 <- lmer(yday ~ temp_90 + I(temp_90^2) + year + mean_elevation + (1 |
  COMID), data = df_mod, REML = FALSE)
m20 <- lmer(yday ~ temp_90 + I(temp_90^2) + year + slope + (1 | COMID),
  data = df_mod, REML = FALSE)
m21 <- lmer(yday ~ temp_90 + I(temp_90^2) + mean_elevation + slope + (1 |
  COMID), data = df_mod, REML = FALSE)
m22 <- lmer(yday ~ stream + year + mean_elevation + (1 | COMID), data = df_mod,
  REML = FALSE)
m23 <- lmer(yday ~ stream + year + slope + (1 | COMID), data = df_mod,
  REML = FALSE)
m24 <- lmer(yday ~ stream + mean_elevation + slope + (1 | COMID), data = df_mod,
  REML = FALSE)
m25 <- lmer(yday ~ year + mean_elevation + slope + (1 | COMID), data = df_mod,
  REML = FALSE)

# four covariates
m26 <- lmer(yday ~ temp_90 + I(temp_90^2) + stream + year + mean_elevation +
  (1 | COMID), data = df_mod, REML = FALSE)
m27 <- lmer(yday ~ temp_90 + I(temp_90^2) + stream + year + slope + (1 |
  COMID), data = df_mod, REML = FALSE)
m28 <- lmer(yday ~ temp_90 + I(temp_90^2) + stream + mean_elevation + slope +
  (1 | COMID), data = df_mod, REML = FALSE)
m29 <- lmer(yday ~ temp_90 + I(temp_90^2) + year + mean_elevation + slope +
  (1 | COMID), data = df_mod, REML = FALSE)
m30 <- lmer(yday ~ stream + I(temp_90^2) + year + mean_elevation + slope +
  (1 | COMID), data = df_mod, REML = FALSE)

# all five covariates
m31 <- lmer(yday ~ temp_90 + I(temp_90^2) + stream + year + mean_elevation +
  slope + (1 | COMID), data = df_mod, REML = FALSE)

```

Table A3.1: AIC selection performance metrics for additive linear models; top 10 of 31 shown.

Model	df	AIC	delta_AIC	R2_marginal	R2_conditional	RMSE	ICC
m26	16	13356.04	0.000	0.785	0.956	2.023	0.796
m31	17	13358.04	1.998	0.785	0.956	2.023	0.795
m27	16	13468.96	112.925	0.737	0.979	2.022	0.922
m16	15	13473.12	117.079	0.729	0.980	2.022	0.926
m29	10	13487.82	131.783	0.727	0.984	2.022	0.942
m19	9	13488.73	132.690	0.726	0.984	2.022	0.943
m7	8	13531.17	175.128	0.660	0.987	2.022	0.962
m20	9	13532.90	176.858	0.660	0.987	2.022	0.962
m17	13	15787.25	2431.210	0.783	0.880	3.112	0.446
m28	14	15789.04	2433.003	0.783	0.880	3.112	0.445

Based on AIC, the best-fitting model was m26, though its improvement in AIC and performance over m31,

the full model which includes `slope`, was modest (Table A3.1). Suggests little benefit to including `slope` as a predictor.

`m27`, which excludes `mean_elevation`, had substantially worse AIC and performance than `m26` and `m31`, indicating that elevation contributes meaningfully to explaining spawn timing variation.

Model `m16`, which excludes both `mean_elevation` and `slope`, had nearly identical predictive accuracy (RMSE) and higher conditional R² compared to `m26` and `m31`, despite a slightly lower (0.73 vs 0.78) marginal R². The 117-point AIC difference between `m16` and `m26` likely reflects subtle improvements in likelihood fit due to topographic covariates.

Visual inspection of partial (model-based) relationships (Figure A3.1 B)) revealed that the modeled elevation effect was inconsistent with ecological expectations.

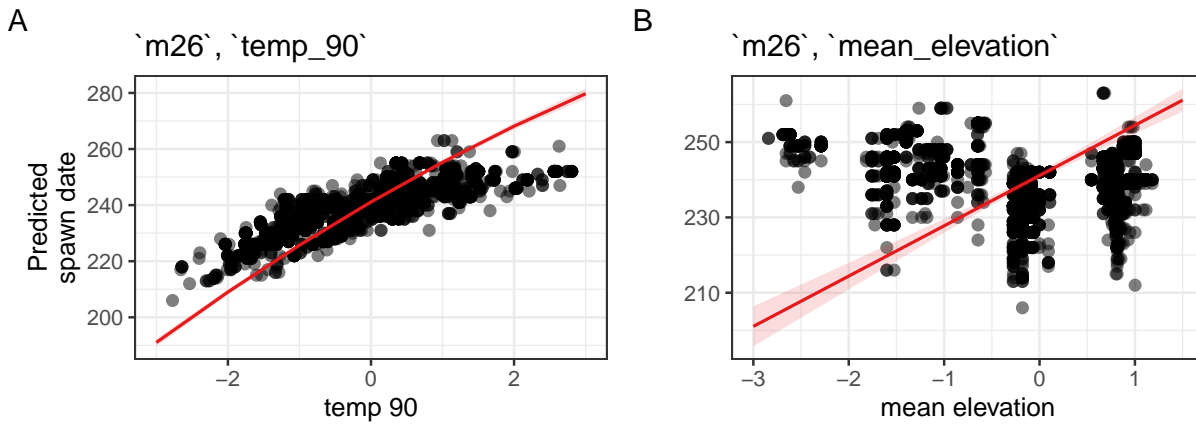


Figure A3.1: Predicted relationship (red line) between spawn date ('yday') and (A) 'temp_90', (B) 'mean_elevation'.

In this case, `m26` is picking up a positive association: after controlling for temperature and stream identity, higher-elevation reaches are predicted to spawn later. This is contrary to the observed negative relationships between elevation, temperature, and spawn timing in several streams (Figure A2.6). This could reflect either (a) a real but subtle ecological effect, or (b) statistical artifact from collinearity/confounding.

- There are some reasons a residual positive elevation effect might make sense:
 - Hydrology and snowmelt: At higher elevations, cooler conditions might delay snowmelt-driven flow cues, potentially pushing back spawning independent of temperature.
 - Population differences: If higher-elevation reaches host subpopulations adapted to shorter growing seasons, they might time spawning later to avoid fry emerging into very harsh winter conditions.
 - Migration lags: Reaches further upstream (which often correspond to higher elevations) could simply take longer for fish to reach, even if temperatures are similar.

But these are second-order hypotheses—we'd need strong ecological justification to lean on them.

- Statistical red flags
 - The positive effect could just as easily be an artifact of collinearity. Elevation and temperature are tightly coupled in your dataset. Once you partial out temperature, the remaining variation in elevation is limited and unstable.

- The fact that predicted vs. observed plots showed inconsistent elevation effects across streams (your Figure elev-plots) suggests this may not be a robust, generalizable signal.

Variance inflation factors (VIFs) from `m26` also indicated moderate collinearity between elevation and stream (VIF = 6.50 and 6.48, respectively). Elevation was strongly confounded with stream identity in our dataset (Figure A2.6), with high-elevation streams showing considerable overlap in spawn timing and temperature.

So, we acknowledge both interpretations:

- Statistically: The positive elevation effect emerges after controlling for temperature, but it is likely confounded by collinearity.
- Ecologically: A true positive effect could be consistent with delayed migration, snowmelt-driven cues, or subpopulation adaptations, but our dataset can't fully disentangle these mechanisms.
- Conclusion: Because the elevation effect runs counter to raw data patterns and shows signs of confounding, we made the conservative decision to omit it from the final model set.

A3.2 Targeted model comparison

We compared our top additive model (`m16`) to a series of increasingly flexible models to evaluate the contribution of random slopes and temperature nonlinearity.

A3.2.1 Random slopes for `temp_90`

To account for potential variation in temperature sensitivity across sites, we extended `m16` to include **COMID-specific random slopes for `temp_90`**, yielding a model with the same fixed effects but with the random structure `(1 + temp_90 | COMID)`. Because the random effects structure differed, we fit both models using restricted maximum likelihood (REML).

```
m16 <- lmer(
  yday ~ temp_90 + I(temp_90^2) + stream + year + (1 | COMID),
  data = df_mod, REML = TRUE
)
m16_rs <- lmer(
  yday ~ temp_90 + I(temp_90^2) + stream + year + (1 + temp_90 | COMID),
  data = df_mod, REML = TRUE
)
```

Table A3.2: Model selection for ‘`m16`’ vs. ‘`m16_rs`’.

Model	df	AIC	delta_AIC	R2_marginal	R2_conditional	RMSE	ICC
<code>m16_rs</code>	17	12948.76	0.000	0.698	0.985	1.781	0.949
<code>m16</code>	15	13459.05	510.283	0.714	0.981	2.022	0.932

The random slope model (`m16_rs`) substantially improved fit ($\Delta\text{AIC} = 510$), reduced RMSE (2.02 → 1.78 days), and slightly increased conditional R^2 (0.981 → 0.985). However, the marginal R^2 declined from 0.714 to 0.698, reflecting a redistribution of explanatory power from fixed to random effects. This shift is expected when site-specific variation in temperature responses is modeled explicitly, and suggests that temperature sensitivity varies meaningfully among stream reaches.

A3.2.2 Partitioning Variation Between Nonlinearity and Heterogeneity

To determine whether the **quadratic temperature term remained necessary** in the presence of random slopes, we re-fit the random slope model with and without $I(temp_90^2)$ using maximum likelihood (ML).

```
m16_rs <- lmer(
  yday ~ temp_90 + I(temp_90^2) + stream + year + (1 + temp_90 | COMID),
  data = df_mod, REML = FALSE
)
m16_rs_noquad <- lmer(
  yday ~ temp_90 + stream + year + (1 + temp_90 | COMID),
  data = df_mod, REML = FALSE
)
```

Table A3.3: Model selection for ‘m16_rs’ vs. ‘m16_rs_noquad’.

Model	df	AIC	delta_AIC	R2_marginal	R2_conditional	RMSE	ICC
m16_rs	17	12965.97	0.000	0.713	0.984	1.782	0.945
m16_rs_noquad	16	12986.41	20.441	0.714	0.984	1.788	0.943

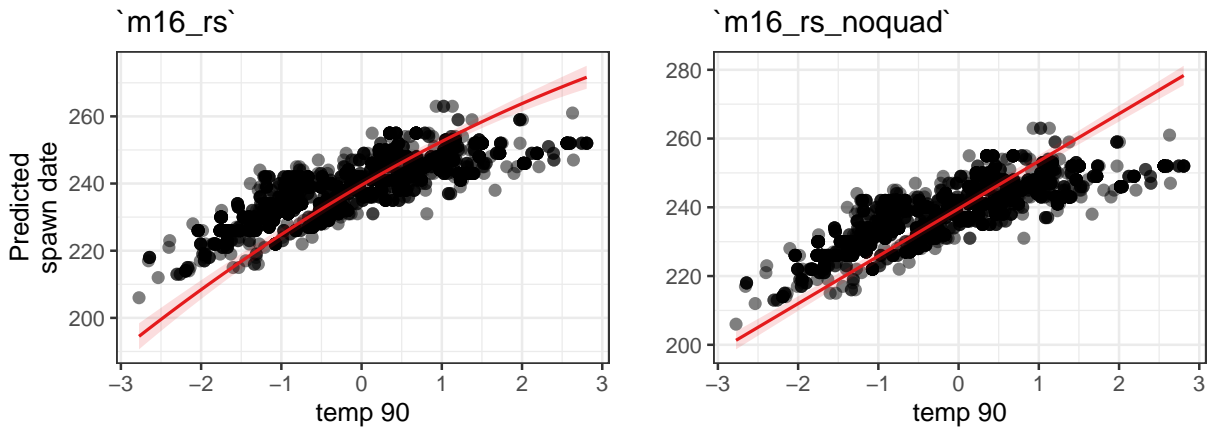


Figure A3.2: Model predictions (red lines) for ‘m16_rs’ and ‘m16_rs_noquad’.

The full model including both quadratic temperature and random slopes (`m16_rs`) outperformed the linear version (`m16_rs_noquad`) by $\Delta AIC = 20.4$, despite only one additional degree of freedom. RMSE and R^2 values were nearly identical, but the full model retained a slightly better fit, particularly at the tails of the temperature distribution. This indicates that while **random slopes capture most of the temperature-related variation**, the quadratic term meaningfully refines the relationship without overfitting or destabilizing the model.

A3.2.3 Summary of random slopes and nonlinearity

To account for site-level variation in thermal sensitivity, we extended this model by allowing COMID-specific random slopes for temperature. This significantly improved model fit ($\Delta AIC = 510$), reduced prediction error (RMSE = 1.78 days), and increased conditional R^2 , indicating that variation in temperature response among stream reaches was substantial and better captured as a random effect.

We then tested whether the quadratic temperature term remained necessary when random slopes were included. The full model with both random slopes and a quadratic temperature effect provided better support ($\Delta AIC = 20.4$) than the linear version, suggesting that each component contributed complementary information. We retained this final model (`m16_rs`) as it provided strong predictive performance while acknowledging both general and site-specific patterns in temperature-spawn timing relationships.

A3.3 Interactions

To assess whether fixed-effect interactions provide additional explanatory power beyond what is captured by random slopes, we tested two models: one with a `temp_90 * stream` interaction (`m201`) and one with a `temp_90 * year` interaction (`m202`). Both were compared to the baseline random slope model with quadratic temperature (`m16_rs`).

```
m201 <- lmer(yday ~ temp_90 * stream + I(temp_90^2) + year + (1 + temp_90 | COMID), data = df_mod, REML = TRUE)
m202 <- lmer(yday ~ temp_90 * year + I(temp_90^2) + stream + (1 + temp_90 | COMID), data = df_mod, REML = TRUE)
```

Table A3.4: Model selection for ‘m201’ vs. ‘m202’.

Model	df	AIC	delta_AIC	R2_marginal	R2_conditional	RMSE	ICC
m202	20	11568.63	0.000	0.620	0.994	1.359	0.985
m201	24	12948.51	1379.886	0.736	0.985	1.786	0.944
m16_rs	17	12965.97	1397.340	0.713	0.984	1.782	0.945

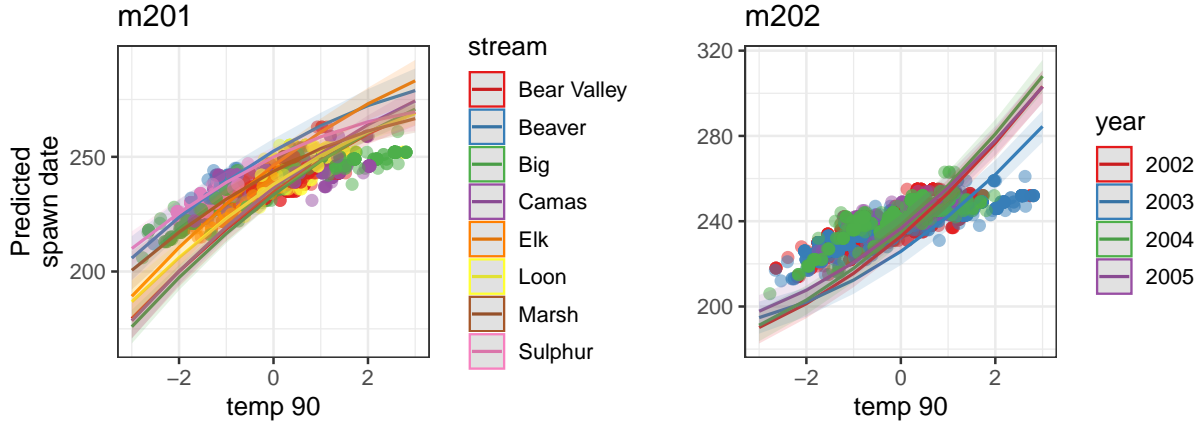


Figure A3.3: Predicted spawn timing.

Model `m202` showed a large AIC improvement ($\Delta AIC = -1397$), but inspection of its predicted effects revealed implausible temperature relationships—specifically, an inverted quadratic curve inconsistent with biological expectations. This suggests overfitting or confounding in the interaction structure.

Model `m201` produced biologically reasonable predictions and modest AIC improvement ($\Delta AIC = -18$), but most interaction terms were non-significant, and variance explained (R^2) remained nearly unchanged. These results indicate that stream-specific variation in thermal sensitivity is already well-captured by the random slope structure.

Given the limited inferential gain and added complexity of the interaction models, we retained `m16_rs` (quadratic temperature with COMID-specific random slopes) as our final model.

A4 Model interpretation

The final model included a linear and quadratic effect of temperature (`temp_90`, `I(temp_90^2)`), additive fixed effects for `stream` and `year`, and a random intercept and slope for temperature by COMID:

```
# final model structure
mod_final <- lmer(
  yday ~ temp_90 + I(temp_90^2) + stream + year + (1 + temp_90 | COMID),
  data = df_mod, REML = TRUE
)
```

This model balances explanatory power, biological realism, and parsimony. It captures both general patterns in spawn timing (via fixed effects) and local deviations in temperature response (via random slopes), and will serve as the basis for diagnostics, prediction, and ecological interpretation.

A4.1 Model parameters and performance

Table A4.1: Parameter estimates for `mod_final`.

Parameter	Coefficient	SE	CI_low	CI_high	p	Effects	Group
(Intercept)	235.09	2.11	230.95	239.22	0.00	fixed	
temp_90	13.90	0.43	13.06	14.74	0.00	fixed	
$I(temp_90^2)$	-0.85	0.15	-1.15	-0.55	0.00	fixed	
streamBeaver	17.41	3.46	10.62	24.19	0.00	fixed	
streamBig	-0.19	2.65	-5.37	5.00	0.94	fixed	
streamCamas	2.30	2.75	-3.08	7.69	0.40	fixed	
streamElk	11.97	3.61	4.88	19.06	0.00	fixed	
streamLoon	2.80	2.68	-2.47	8.06	0.30	fixed	
streamMarsh	7.93	2.87	2.30	13.56	0.01	fixed	
streamSulphur	14.69	3.06	8.69	20.69	0.00	fixed	
year2003	-5.00	0.12	-5.23	-4.77	0.00	fixed	
year2004	2.77	0.12	2.53	3.01	0.00	fixed	
year2005	3.68	0.15	3.38	3.98	0.00	fixed	
SD (Intercept)	7.05	NA	NA	NA	NA	random	COMID
SD (temp_90)	3.55	NA	NA	NA	NA	random	COMID
Cor (Intercept~temp_90)	-0.23	NA	NA	NA	NA	random	COMID
SD (Observations)	1.83	NA	NA	NA	NA	random	Residual

Table A4.2: Model performance for `mod_final`.

AIC	AICc	BIC	R2_conditional	R2_marginal	ICC	RMSE	Sigma
12948.76	12948.97	13050.96	0.9845502	0.6979933	0.9488428	1.780765	1.833613

Parameter estimates (Table A4.1) indicate a significant nonlinear effect of temperature on spawn timing, with the quadratic term (-0.85) confirming a concave-down relationship—i.e., spawn timing advances with increasing temperature, but levels off at high temperatures.

Most stream and year effects were significant, capturing expected spatiotemporal structure in spawn timing. Notably, Big, Camas, and Loon were not significantly different from the reference level (Bear Valley).

The random effects structure reveals substantial variation across COMIDs. The standard deviation for random intercepts ($\sqrt{\sigma^2} = 7.05$) and random slopes for `temp_90` ($\sqrt{\sigma^2} = 3.55$) indicates strong spatial heterogeneity in both baseline timing and temperature sensitivity (Table A4.1). The intraclass correlation (ICC) was high (0.95), reflecting strong grouping structure at the COMID level (Table A4.2).

Model fit was excellent: the marginal R^2 (variance explained by fixed effects) was 0.698, and the conditional R^2 (fixed + random effects) was 0.985 (Table A4.2). This suggests that the majority of explanatory power is derived from spatially varying thermal responses captured by the random slopes, with additional structure provided by the fixed effects.

A4.2 Residual diagnostics

Model diagnostics for the final model were generally strong (Figure A4.1). The posterior predictive check shows excellent agreement between the observed and model-predicted distributions of spawn timing, with overlapping density curves and no major deviations.

Plots of linearity and homoscedasticity indicate acceptable model performance. While the residual vs. fitted plot shows a slight trend, it does not appear strong enough to invalidate model assumptions. The spread of residuals is approximately constant across fitted values, though there is minor funneling at the lower end, likely reflecting skew in early spawn dates.

Influential observations are limited. A few data points exceed standard influence thresholds ($|z_{standardized}| > 2$ and high leverage), but none are extreme enough to warrant removal, and their leverage is modest. The model appears robust to outliers.

Collinearity is low: variance inflation factors (VIFs) for all fixed effects are well below the conservative threshold of 5, suggesting little concern about multicollinearity.

The normal Q-Q plot of residuals shows slight right-skew and some heavy tails, but the distribution is reasonably close to normal. Similarly, random effect Q-Q plots for intercepts and slopes show mostly linear trends with slight deviation at the tails, indicating acceptable assumptions for the mixed-effects structure.

Overall, the model shows no violations of key assumptions and is suitable for inference and prediction.

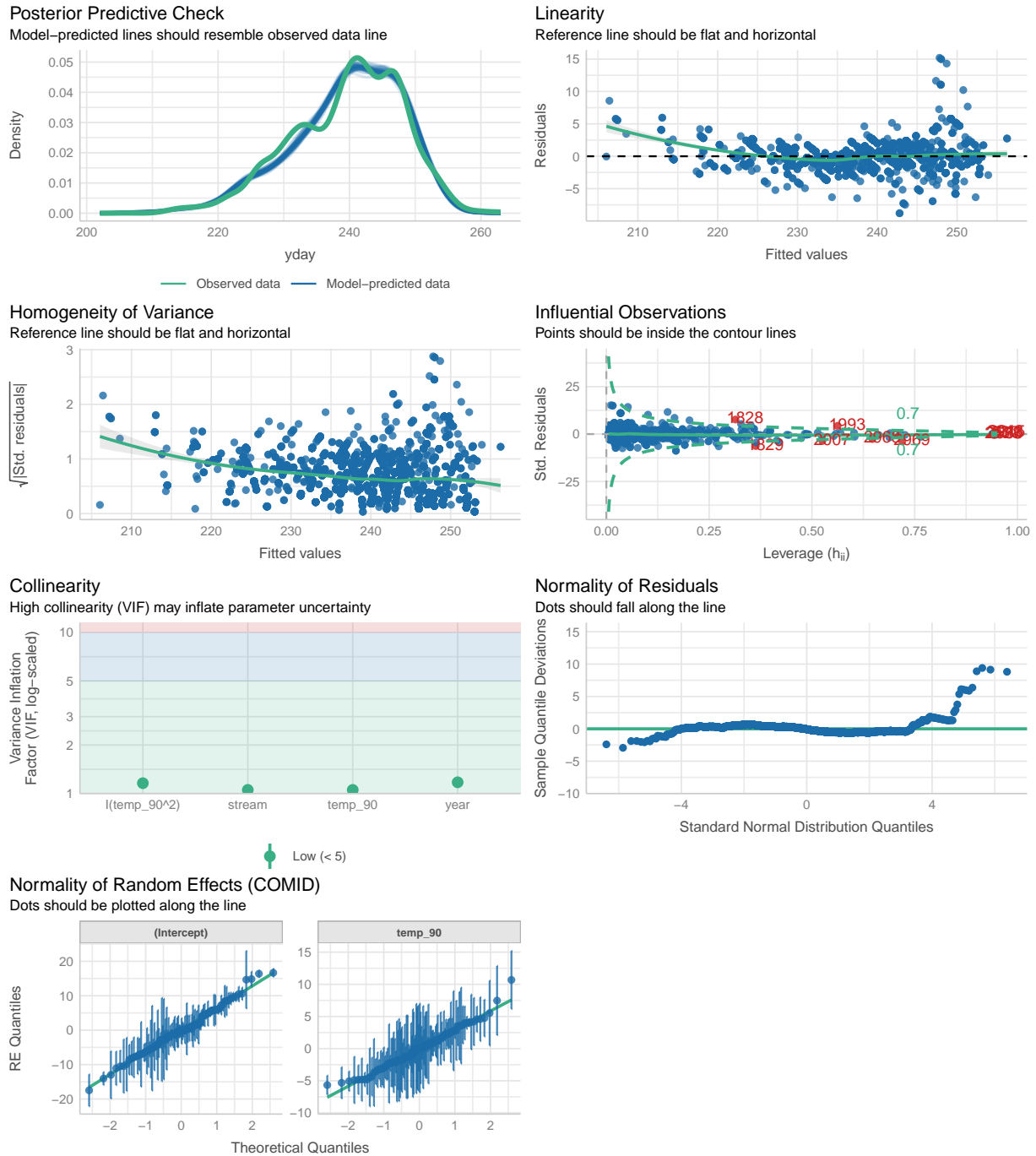


Figure A4.1: Residual diagnostics for mod_final.

A4.3 Predictions against original data

Model predictions closely matched observed spawn timing, with predicted values aligning well along the 1:1 line (Figure A4.2). This supports strong overall model fit.

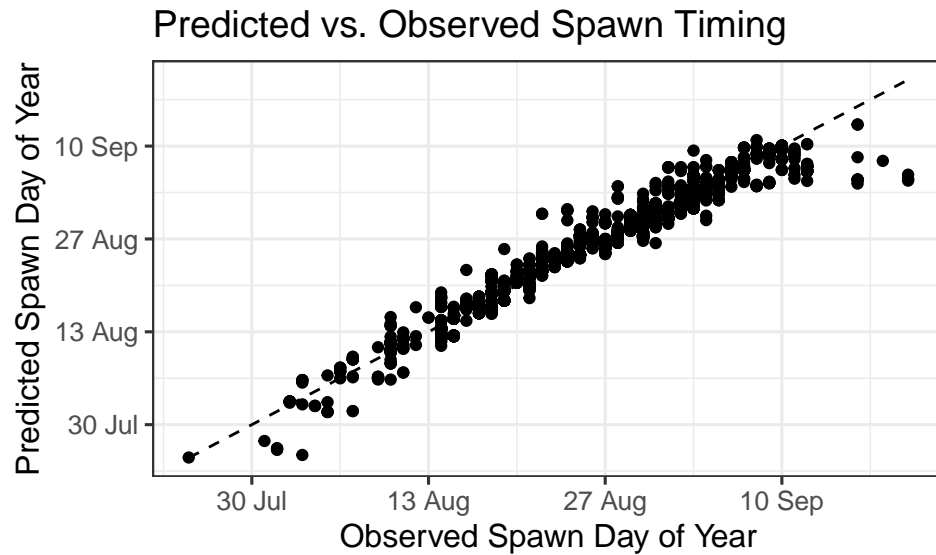


Figure A4.2: Predicted vs. observed spawn timing for Chinook Salmon across all years and streams. The dashed line shows the 1:1 line. Points represent individual redd observations.

A4.4 Population-level effects

A4.4.1 Marginal means and contrasts of yday at each factor level

We estimated marginal mean of yday at each factor level, averaging over the random effects, to provide an overall estimate of the effect in the population (Figure A4.3).

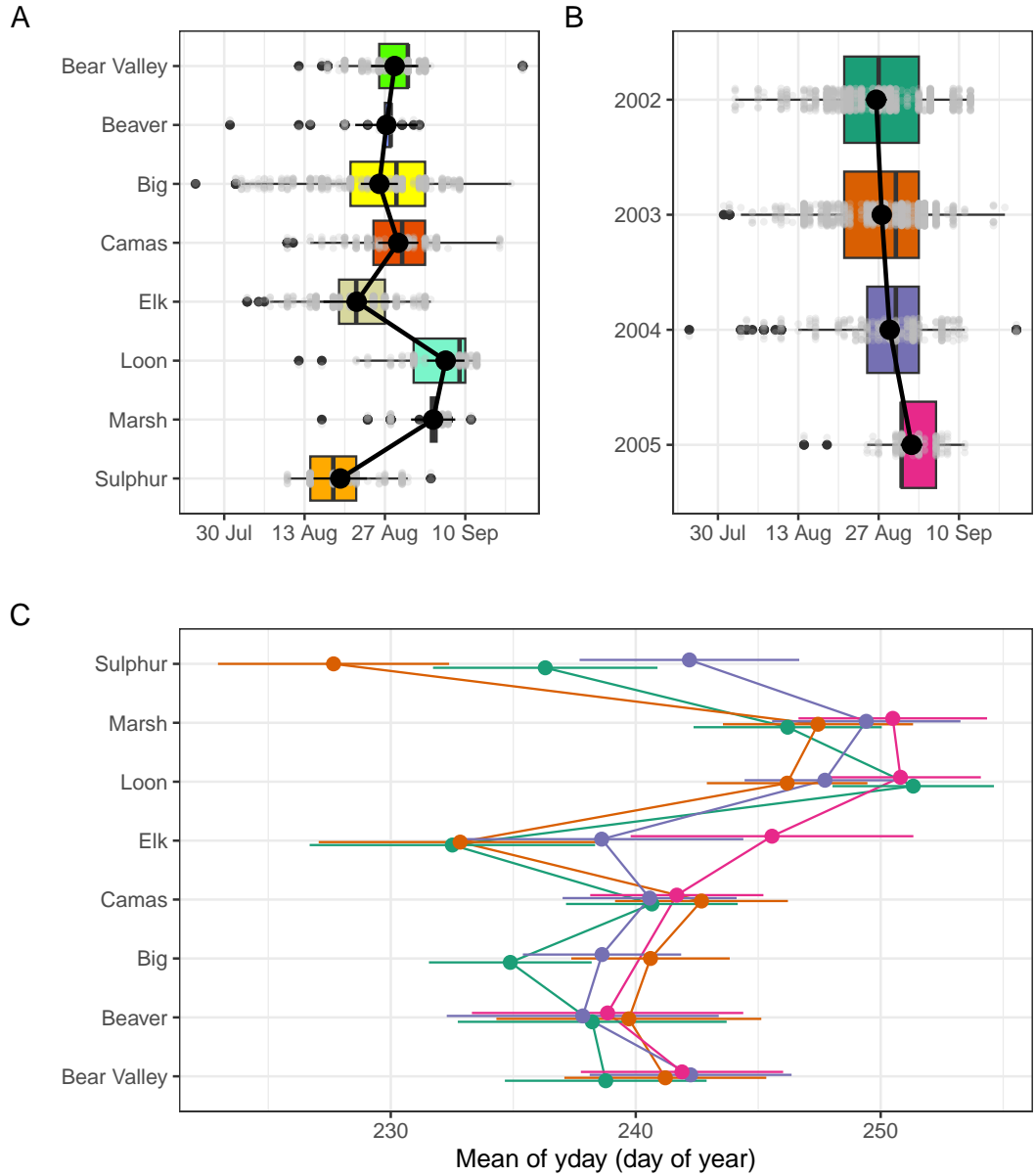


Figure A4.3: Predicted mean spawn dates by stream (A), year (B) and stream and year (C), from the final mixed-effects model. Black points with black lines (A, B), and colored points with horizontal lines (C) represent estimated marginal means and 95% confidence intervals. Boxplots in panels A and B show the distribution of observed redd counts by group, with individual data points in grey. The modeled predictions represent marginal means accounting for fixed effects and averaged over random effects.

Significant differences in spawn timing were observed between many stream pairs (Table A4.3), particularly involving Loon (later spawning) and Sulphur (earlier spawning). For example, fish in Loon spawned significantly later than in Bear Valley, Camas, and Elk, while Sulphur exhibited significantly earlier timing than all other streams except Elk. These patterns reflect spatial heterogeneity in temperature and elevation across streams that is not fully captured by fixed effects alone.

There was a clear trend toward later spawning over the four-year period (Table A4.4). Spawning in 2005 occurred significantly later than in all previous years. Differences between 2002 and 2003 were not statistically

Table A4.3: Pairwise contrasts among stream effects on predicted spawn timing. Contrasts represent estimated differences in predicted spawn day of year between streams from the final model. Positive values indicate later predicted spawn timing in the first stream compared to the second. P-values are uncorrected.

Level1	Level2	Difference	SE	CI_low	CI_high	t	df	p
Beaver	Bear Valley	-1.43	3.47	-8.23	5.38	-0.41	2999	0.68
Big	Bear Valley	-2.66	2.66	-7.88	2.56	-1.00	2999	0.32
Camas	Bear Valley	0.63	2.75	-4.77	6.03	0.23	2999	0.82
Elk	Bear Valley	-6.60	3.62	-13.71	0.50	-1.82	2999	0.07
Loon	Bear Valley	8.90	2.68	3.64	14.15	3.32	2999	0.00
Marsh	Bear Valley	6.72	2.87	1.08	12.35	2.34	2999	0.02
Sulphur	Bear Valley	-9.47	3.16	-15.66	-3.28	-3.00	2999	0.00
Big	Beaver	-1.23	3.18	-7.46	4.99	-0.39	2999	0.70
Camas	Beaver	2.06	3.27	-4.35	8.46	0.63	2999	0.53
Elk	Beaver	-5.18	4.01	-13.04	2.69	-1.29	2999	0.20
Loon	Beaver	10.33	3.24	3.98	16.67	3.19	2999	0.00
Marsh	Beaver	8.14	3.41	1.46	14.82	2.39	2999	0.02
Sulphur	Beaver	-8.04	3.54	-14.98	-1.10	-2.27	2999	0.02
Camas	Big	3.29	2.40	-1.42	8.00	1.37	2999	0.17
Elk	Big	-3.94	3.35	-10.51	2.62	-1.18	2999	0.24
Loon	Big	11.56	2.35	6.95	16.16	4.92	2999	0.00
Marsh	Big	9.38	2.57	4.33	14.42	3.64	2999	0.00
Sulphur	Big	-6.81	2.78	-12.26	-1.36	-2.45	2999	0.01
Elk	Camas	-7.23	3.43	-13.97	-0.50	-2.11	2999	0.04
Loon	Camas	8.27	2.45	3.47	13.06	3.38	2999	0.00
Marsh	Camas	6.09	2.66	0.87	11.30	2.29	2999	0.02
Sulphur	Camas	-10.10	2.91	-15.80	-4.40	-3.47	2999	0.00
Loon	Elk	15.50	3.40	8.84	22.17	4.56	2999	0.00
Marsh	Elk	13.32	3.56	6.34	20.30	3.74	2999	0.00
Sulphur	Elk	-2.87	3.71	-10.14	4.41	-0.77	2999	0.44
Marsh	Loon	-2.18	2.57	-7.23	2.87	-0.85	2999	0.40
Sulphur	Loon	-18.37	2.91	-24.07	-12.66	-6.31	2999	0.00
Sulphur	Marsh	-16.19	3.10	-22.27	-10.10	-5.22	2999	0.00

significant, but later years (2004 and especially 2005) were associated with a progressive delay in mean spawn timing. This temporal shift likely reflects interannual variability in temperature and flow conditions.

Table A4.4: Pairwise contrasts among year effects on predicted spawn timing. Contrasts represent estimated differences in predicted spawn day of year between years from the final model. Positive values indicate later spawning in the first year compared to the second. P-values are uncorrected.

Level1	Level2	Difference	SE	CI_low	CI_high	t	df	p
2003	2002	0.97	0.57	-0.15	2.10	1.70	2999	0.09
2004	2002	2.35	0.65	1.07	3.62	3.61	2999	0.00
2005	2002	6.18	0.61	4.98	7.37	10.17	2999	0.00
2004	2003	1.37	0.61	0.18	2.56	2.26	2999	0.02
2005	2003	5.20	0.71	3.80	6.60	7.28	2999	0.00
2005	2004	3.83	0.87	2.11	5.54	4.38	2999	0.00

A4.4.2 Estimating response vs. relation

To visualize the model's predictions across the temperature gradient, we estimated the relationship between spawn timing and 90-day pre-spawn mean temperature (`temp_90`) for different groupings: overall, by stream, and by year. This approach allows us to assess both general trends and context-specific responses.

Stream-specific predictions (see plot suggestion below) show a consistent pattern: spawn timing increases nonlinearly with 90-day mean stream temperature, leveling off at high temperatures. This plateau is consistent with biological expectations, as spawning may be constrained by environmental or physiological thresholds. Stream-to-stream variation in predicted timing reflects both fixed stream effects and COMID-specific random intercepts and slopes.

Year-specific predictions similarly show consistent thermal responses across years, with modest offsets in average spawn timing due to year effects. These predictions further validate the model's generalizability and temporal consistency.

In addition, a combined stream-by-year plot (e.g., facet grid) confirms that the final model captures heterogeneity in both space and time without overfitting. Lines track the raw data closely across groups, particularly in mid-range temperatures where most observations are concentrated.

Together, these plots indicate that the final model effectively captures both nonlinear temperature effects and spatial variation in thermal sensitivity, while maintaining interpretability and predictive strength.

When stratified by stream and year, predictions captured both the nonlinear temperature response and variation in baseline spawn timing across sites and years (Figure A4.4). The curvature was consistent across years, while intercept shifts reflected known spatial patterns (e.g., later spawning in warmer, downstream reaches). These results confirm that the model accurately describes both average and context-specific phenological responses to temperature.

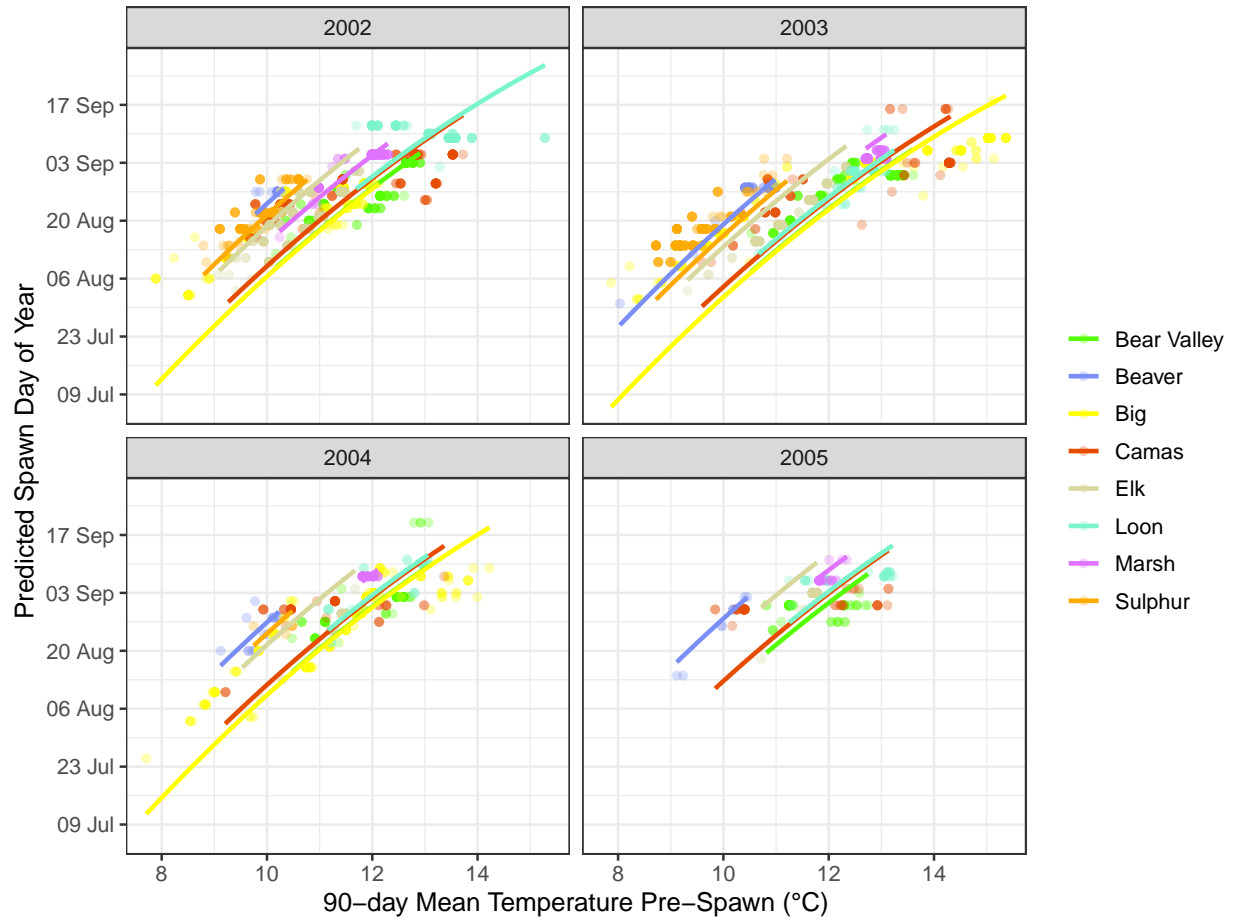


Figure A4.4: Predicted relationship between spawn timing and 90-day pre-spawn mean temperature by stream and year. Lines represent model predictions from the final mixed-effects model. Colored points show observed redd timing, shaded ribbons represent 95% confidence intervals for predictions.

A4.5 Group-level effects (deviations from fixed effects)

Random intercepts and slopes varied considerably among COMIDs, reflecting spatial heterogeneity in both average spawn timing and thermal sensitivity (Figure A4.5A). We found substantial spread in intercepts, indicating variability in baseline spawn timing among reaches. Random slopes for temp_90 likewise varied meaningfully, showing that temperature–spawn timing relationships were not constant across space. Sites with earlier average spawn timing (lower intercepts) generally exhibited stronger positive responses to temperature (higher slopes), whereas later-spawning sites tended to present weaker temperature effects—a pattern evident in the weak negative correlation between intercepts and slopes ($r = -0.2$; Figure A4.5B). These findings highlight spatial heterogeneity in phenological flexibility, with potential implications for how different Middle Fork salmon populations may respond to ongoing climate change.

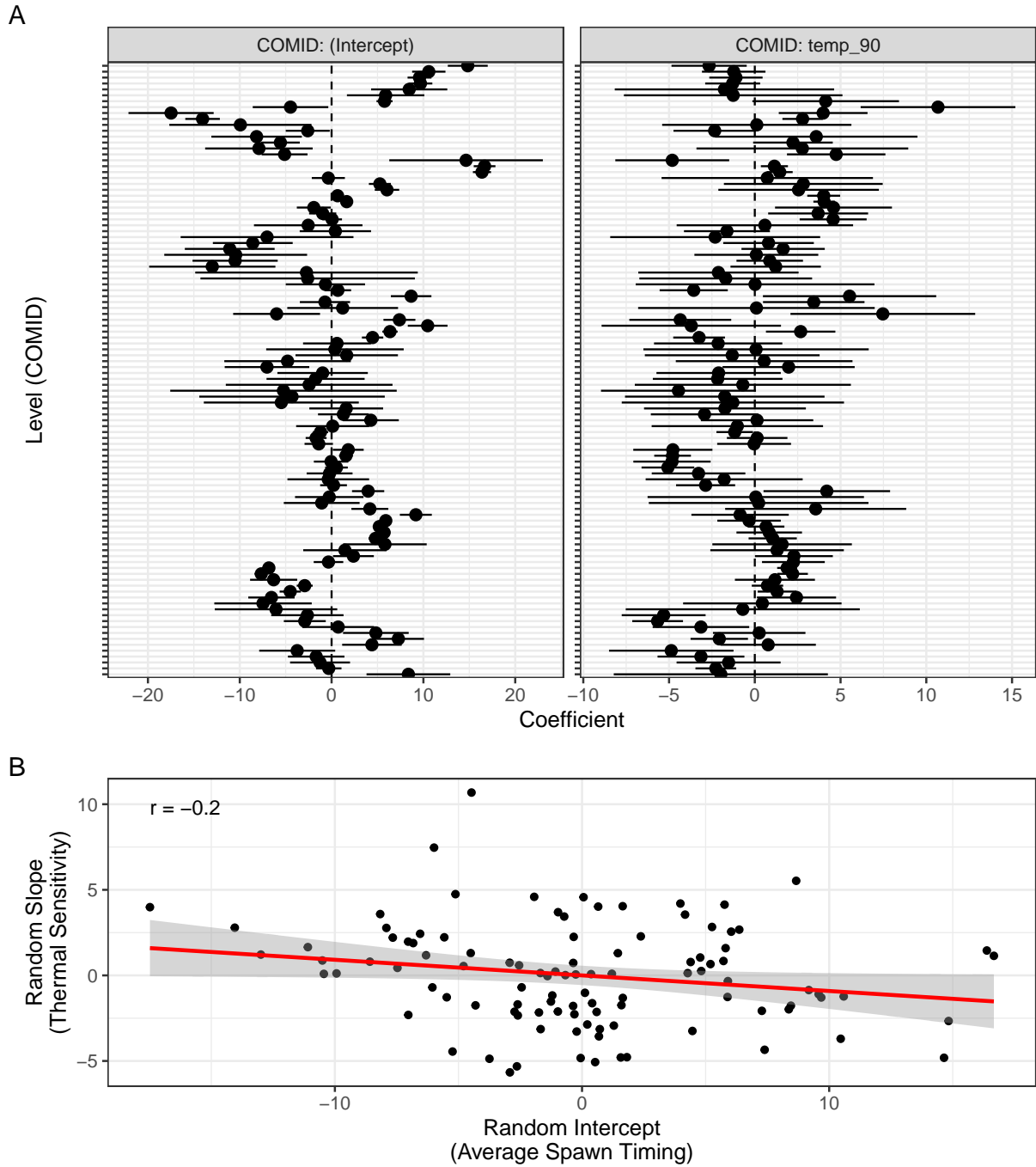


Figure A4.5: (A) COMID-specific random parameter estimates for intercepts (left) and slopes (right). Points represent best linear unbiased predictions (BLUPs) from the final model, with horizontal bars indicating ± 1.96 standard errors. (B) Correlation between random intercepts and slopes for 90-day temperature across COMIDs. Each point represents a stream reach (COMID).

Figure 7 further illustrates this variability across scales, summarizing the distribution of random intercepts and slopes by stream (panel A) and the corresponding predicted temperature–spawn timing relationships for individual reaches (panel B). COMID-level variation in intercepts and slopes reveals substantial spatial het-

erogeneity in both average timing and thermal sensitivity, with some streams showing greater within-stream variability than others. While the overall relationship between 90-day pre-spawn temperature and spawn timing is positive and nonlinear, the strength and shape of this response vary among reaches, likely reflecting fine-scale differences in hydrology, geomorphology, or biological composition. Despite this heterogeneity, the consistency of the population-level trend underscores the biological relevance of temperature as a key cue structuring spawn timing in Middle Fork Chinook Salmon populations.

(Figure ??).

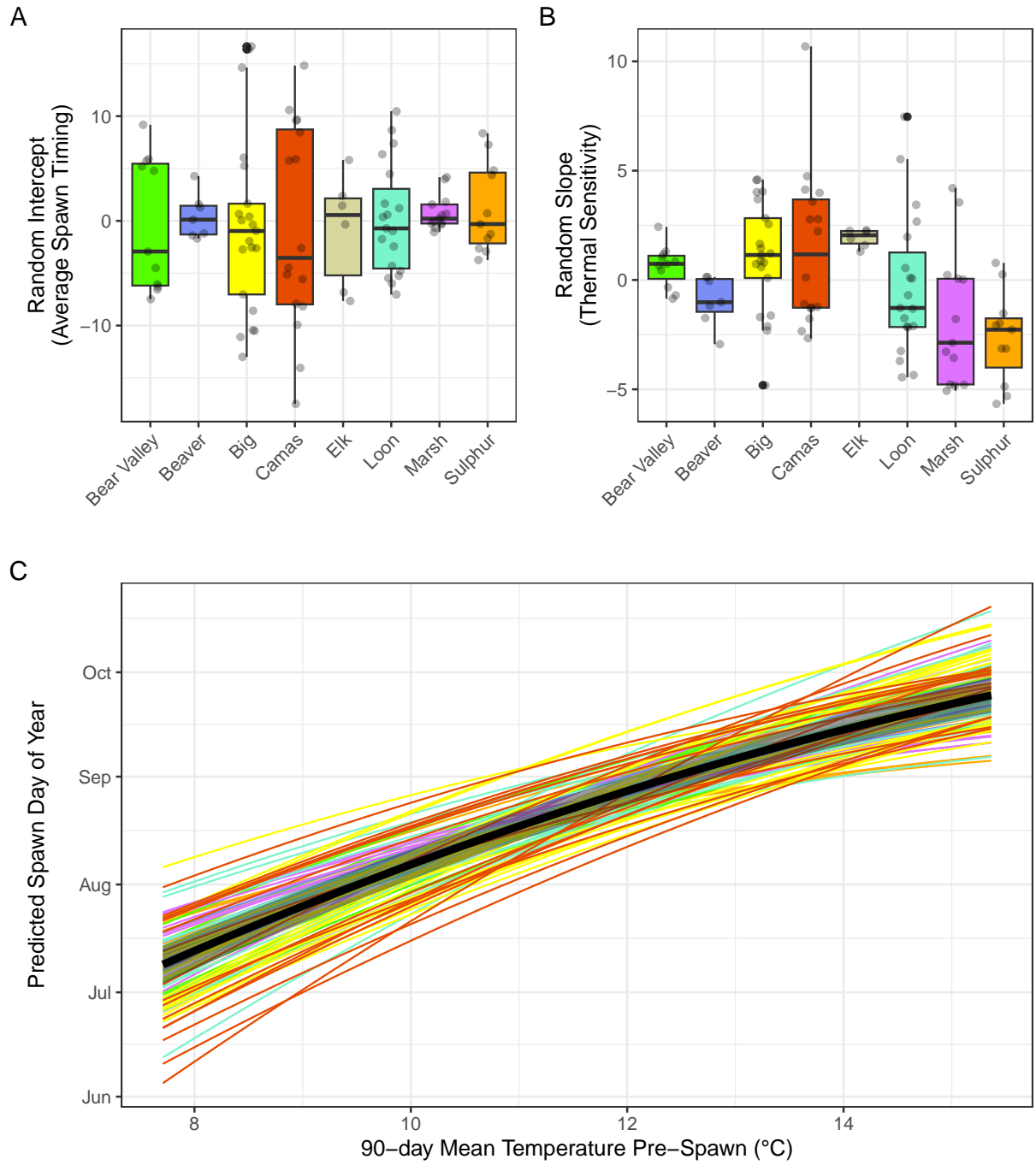


Figure A4.6: Variation in COMID- and stream-level thermal sensitivity and predicted spawn timing relationships. (A) Boxplots of random intercepts and slopes for 90-day pre-spawn temperature by stream. Each box represents the distribution of best linear unbiased predictions (BLUPs) for COMID-level intercepts (average spawn timing) or slopes (thermal sensitivity). (B) Predicted spawn timing by 90-day pre-spawn temperature and COMID. Each line represents the predicted relationship for a specific COMID, colored by stream. The black line and shaded ribbon denote the population-level mean and 95% confidence interval.